TITLE:

Evolution and diversification of the momilactone biosynthetic gene cluster in the genus *Oryza*

AUTHORS:

Santiago Priego-Cubero[1], Tomonobu Toyomasu[2], Michael Gigl[3], Youming Liu[4], Yuto Hasegawa[2], Hideaki Nojiri[4], Corinna Dawid[3], Kazunori Okada[4], Claude Becker[1,*]

[1] Faculty of Biology, Ludwig-Maximilians-Universität München, 82152 Martinsried, Germany

[2] Faculty of Agriculture, Yamagata University, Tsuruoka, Yamagata, 997-8555, Japan

[3] Professorship for Functional Phytometabolomics, TUM School of Life Sciences, Technical University of Munich, Lise-Meitner-Str. 34, 85354 Freising

[4] Agro-Biotechnology Research Center (AgTECH), Graduate School of Agricultural and Life Sciences (GSALS), The University of Tokyo, Tokyo, 113-8657, Japan

[*] To whom correspondence should be addressed: claude.becker@lmu.de

ORCIDs:

Santiago Priego Cubero: 0009-0006-5209-7942

Kazunori Okada: 0000-0001-7321-7911

Michael Gigl: 0000-0002-5617-9236

Corinna Dawid: 0000-0001-5342-2600

Claude Becker: 0000-0003-3406-4670

ABSTRACT

Plants are master chemists and collectively are able to produce hundreds of thousands of different organic compounds. The genes underlying the biosynthesis of many specialized metabolites are organized in biosynthetic gene clusters (BGCs), which is hypothesized to ensure their faithful co-inheritance and to facilitate their coordinated expression. In rice, momilactones are diterpenoids that act in plant defence and various organismic interactions. Many of the genes essential for momilactone biosynthesis are grouped in a BGC. Here, we apply comparative genomics of diploid and allotetraploid *Oryza* species to reconstruct the species-specific architecture, evolutionary trajectory, and sub-functionalisation of the momilactone biosynthetic gene cluster (MBGC) in the *Oryza* genus. Our data show that the evolution of the MBGC is marked by lineage-specific rearrangements and gene copy number variation, as well as by occasional cluster loss. We identified a distinct cluster architecture in *O. coarctata*, which represents the first instance of an alternative architecture of the MBGC in *Oryza* and strengthens the idea of a common origin of the cluster in *Oryza* and the distantly related genus *Echinochloa*. Our research illustrates the evolutionary and functional dynamics of a biosynthetic gene cluster within a plant genus.

INTRODUCTION

Biosynthetic gene clusters and their evolution

With more and more plant reference genome assemblies becoming available, biosynthetic gene clusters (BGCs), i.e., the co-localization of often phylogenetically unrelated genes that participate in the same biosynthetic cascade of specialized metabolites, have emerged as a common feature of genomic organization in plants (Polturak et al., 2022b). BGCs are postulated to confer evolutionary advantages because they facilitate coordinated gene expression, enable the reliable coinheritance of genes involved in the same metabolic pathway (thereby preventing the accumulation of toxic intermediates), or facilitate the formation of metabolons (Nützmann et al., 2016). However, the mechanisms by which such non-orthologous genes become localized in the same genomic region and act in the same biosynthetic pathway are still poorly understood. Currently, the most common model proposes that they have formed through a series of events that is driven by both positive and negative selection pressure, starting with gene duplication, followed by neo-functionalization, and ultimately relocation. In some cases, this process appears to have been mediated by transposable elements (Polturak et al., 2022b; Smit and Lichman, 2022).

Biological functions of rice phytoalexins, labdane-related diterpenoids and momilactones

Phytoalexins are low-molecular-mass specialized plant metabolites that are often produced under biotic and abiotic stress conditions (Ahuja et al., 2012). In rice (*Oryza sativa*), the major phytoalexins are a group of labdane-related diterpenoids (reviewed in Toyomasu et al., 2020), which derive from the cyclization of geranylgeranyl diphosphate (GGPP) into *ent*, *syn*, or normal stereoisomers of copalyl diphosphate (CDP) by the class II diterpene synthases Copalyl Diphosphate Synthases (CPSs). The biosynthesis of these metabolites has evolved from that of gibberellins (GAs), *ent* labdane-related diterpenoids themselves, through duplication and neofunctionalization of core biosynthetic enzymes (Zi et al., 2014). Several *ent* and *syn* (but not normal) rice labdane-related diterpenoids have been identified, including momilactones A and B, phytocassanes A to F, and oryzalexins (A to F, and S) (Toyomasu et al., 2020; Zi et al., 2014). Notably, momilactone A and, more prominently, momilactone B have a strong allelopathic activity, i.e., they inhibit the germination and growth of nearby plants upon being released by the rice plants into the soil (Kato et al., 1973; Kato-Noguchi et al., 2010; Serra Serra et al. 2021). Both compounds accumulate in rice husks but are also exuded from the roots (Kato-Noguchi et al., 2010; Kato-Noguchi and Ino, 2003).

Biosynthesis of momilactones and clustering of momilactone genes

Momilactone biosynthesis starts with the cyclization of GGPP into *syn*-copalyl diphosphate (*syn*-CDP), catalysed by the Copalyl Diphosphate Synthase 4 (CPS4) (Otomo et al., 2004b; Xu et al., 2004). *syn*-CDP is further cyclized into *syn*-pimara-7,15-diene by *ent*-kaurene synthase-like 4 (KSL4), a class I diterpene synthase (Otomo et al., 2004a; Wilderman et al., 2004). Because *syn*-CDP is also a substrate for oryzalexin S biosynthesis, the KSL4-mediated cyclization is the first truly dedicated step towards momilactone production (Tamogani et al., 1993). 9βH-pimara-7,15-diene undergoes several oxidation steps, catalysed first by cytochrome P450 (CYP) monooxygenases CYP76M8 and CYP99A3, followed by the short-chain alcohol dehydrogenase MOMILACTONE A SYNTHASE (MAS) and CYP701A8, to yield momilactone A (De La Peña and Sattely, 2021; Kitaoka et al., 2021). CYP76M14 catalyses the final hydroxylation of C20, leading to spontaneous closure of the hemi-acetal ring and forming momilactone B (De La Peña and Sattely, 2021). Among the biosynthetic genes, *CPS4*, *KSL4*, and the paralogs *CYP99A2/3* and *MAS1/2* are co-localized on chromosome 4 in a momilactone biosynthetic gene cluster (MBGC) (Miyamoto et al., 2016; Shimura et al., 2007). However, not all genes required for momilactone biosynthesis are contained in the MBGC:

91 *CYP76M8* is located on chromosome 2 and is part of another BGC that is required for
92 phytocassane and oryzalexin production (Okada, 2011; Kitaoka et al., 2021), while *CYP701A8*
93 and *CYP76M14* are located on chromosomes 6 and 1, respectively (De La Peña and Sattely,
94 2021).

95 *Evolution of the momilactone biosynthetic gene cluster in Oryza*

96 The *Oryza* genus (belonging to the *Poaceae* family) consists of 27 known species with 11
97 different genome types (classified based on cytogenetics and genetic hybridization studies):
98 6 diploids (n = 12; AA, BB, CC, EE, FF and GG) and 5 allotetraploids (n = 24; BBCC, CCDD,
99 HHJJ, HHKK and KKLL) (Ge et al., 1999; Lu et al., 2009). The MBGC was established in
100 *Oryza* before the domestication of rice (*O. sativa*; AA) (Miyamoto et al., 2016). It is highly
101 conserved among AA and BB genome type *Oryza* species, while only a partial cluster exists
102 in the early-divergent *Oryza* species *O. brachyantha* (FF), which harbours only two clustered
103 *CYP99A2/3* paralogs (Miyamoto et al., 2016). Because the MBGC is incomplete in *O.*
104 *brachyantha*, it likely evolved prior to the divergence of the BB lineage in *Oryza* (Miyamoto et
105 al., 2016). Due to the limited availability of genome assemblies from species positioned
106 between *O. brachyantha* and *O. punctata* in the phylogenetic tree, it has remained unclear
107 whether the MBGC was restricted to species of the AA and BB lineages. Alternatively, the
108 MBGC could have been lost specifically in the *O. brachyantha* lineage and might be present
109 in other *Oryza* lineages. Lastly, the presence and configuration of the MBGC have not yet
110 been studied in any of the allotetraploid *Oryza* species, and it therefore remains unknown if
111 the cluster is present in both their sub-genomes.

112 *Momilactone biosynthetic gene cluster in other species*

113 Studies of the MBGC have not been limited to the *Oryza* genus; some have expanded into the
114 wider *Poaceae* family. *Poaceae* encompass twelve subfamilies, of which nine belong to two
115 core clades: BOP and PACMAD. The BOP clade comprises Bambusoideae, Oryzoideae
116 (including *Oryza*), and Pooideae (including the *Triticeae* tribe); the PACMAD clade consists of
117 Panicoideae, Aristidoideae, Chloridoideae, Micrairoideae, Arundinoideae, and
118 Danthonioideae (Soreng et al., 2017). The MBGC is not restricted to the *Oryza* genus and has
119 been identified through phylogenomic methods in species belonging to the PACMAD clade,
120 specifically in the Panicoideae and Chloridoideae subfamilies (Wu et al., 2022a). However, it
121 remains uncertain whether these species actually produce momilactones or other types of
122 labdane-related diterpenoids. *Echinochloa crus-galli* (Panicoideae), a prevalent weed
123 associated with rice cultivation, is the only species confirmed to produce momilactone A

124 (Kraehmer et al., 2016; Wu et al., 2022a). Interestingly, *E. crus-galli* exhibits a distinct MBGC
125 architecture, including an additional cytochrome P450 (*EcCYP76L11*) (Guo et al., 2017;
126 Kitaoka et al., 2021). EcCYP76L11, similarly to CYP76M8 in *Oryza sativa*, can catalyse the
127 conversion of *syn*-pimaradiene into 6β-hydroxy-*syn*-pimaradiene (Kitaoka et al., 2021).
128 Despite the shared origin of the MBGC in *Oryza* and *Echinochloa*, the *CYP76L11* gene has
129 not been identified in the MBGC or the genome of any *Oryza* species (Wu et al., 2022a).

130 Here, we studied the presence, architecture, and evolution of the MBGC in cultivated rice and
131 wild relatives from the *Oryza* genus by mining recently published genome assemblies. Our
132 study shows that the MBGC is not restricted to species of the AA and BB lineages; we identify
133 MBGC-like clusters in *Oryza* CC species and in one of the respective sub-genomes of the
134 tetraploid species *O. alta* as well as in *O. coarctata*, a basal lineage in the *Oryza* phylogeny.
135 We also show that the gene cluster was lost in several intermediate genome types. While
136 momilactone A was detectable in all species harbouring the cluster, our data indicate that
137 momilactone B production might have been a more recent innovation that emerged after the
138 branching off of the KK genome type. In the *O. coarctata* MBGC, we identified an additional
139 CYP that is different from the canonical *O. sativa* CYP99A2/3 and for which a corresponding
140 ortholog could be found only in the MBGC of *E. crus-galli*, altogether suggesting the existence
141 of an early ancestral cluster. In summary, our study shows how a biosynthetic gene cluster
142 diversified within a plant genus while largely maintaining its biosynthetic function.

143 RESULTS

144 *The momilactone biosynthetic gene cluster is prevalent throughout the Oryza genus*

145 Among the 11 different genome types within the genus *Oryza*, the MBGC has been extensively
146 studied in only 3 lineages. The cluster exhibits a high level of conservation among *Oryza*
147 species of the AA and BB genome groups, whereas it is incomplete in the FF species *O.*
148 *brachyantha* (Figure 1b) (Miyamoto et al., 2016). To better understand the evolution of MBGC
149 in the different *Oryza* lineages, we mined newly published genome assemblies
150 (Supplementary Table 1) for the presence and location of the MBGC (see methods for details).
151 Our analysis included genomes of the diploid species *O. officinalis*, *O. eichingeri*, *O. rhizomatis*
152 (all CC), *O. australiensis* (EE), and *O. granulata* (GG), as well as of the allotetraploid species
153 *O. alta* (CCDD) and *O. coarctata* (KKLL). We also included *Leersia perrieri* as an outgroup to
154 *Oryza* in our analyses. We used OrthoFinder (Emms and Kelly, 2019) to identify orthogroups
155 containing putative *O. sativa* momilactone biosynthetic genes (Figure 1a). Based on

156 phylogenetic relationships between the set of genes in each orthogroup, we considered as
157 homologs those genes that belonged to the same clade as the *O. sativa* momilactone
158 biosynthetic genes (Supplementary Figures 1-4). We further mined the genomic regions
159 upstream and downstream of the identified homologs to confirm their organization in a
160 genomic cluster.

161 We detected the MBGC in the CC genome species *O. officinalis*, and the corresponding genes
162 across different scaffolds of two other CC species, *O. eichingeri*, and *O. rhizomatis*. Within the
163 CC lineage, gene copy numbers varied, and for some genes we found signatures of species-
164 dependent duplications. In *O. officinalis* (CC), the cluster (~385 kb in length) was located on
165 chromosome 4 and contained *CPS4*, *MAS*, two copies of *KSL4*, and two *CYP99A2/3* orthologs
166 (Figure 1b). In *O. eichingeri* and *O. rhizomatis* (both CC), we identified orthologs of *CPS4*,
167 *MAS*, two copies of *KSL4*, and *CYP99A2/3*; *O. eichingeri* carried two copies each for
168 *CYP99A2/3* and *MAS*, with the second copy of the latter appearing pseudogenic (Figure 1b).
169 However, in the scaffold-level assemblies of *O. eichingeri* and *O. rhizomatis*, we found these
170 genes localized on different scaffolds. In *O. rhizomatis*, the *CYP99A2/3* and one of the *KSL4*
171 paralogs co-occurred on Scaffold2280, *CPS4* and the other *KSL4* paralog on Scaffold1491
172 (Figure 1b). In agreement with the presence of the cluster in all CC species, we identified a
173 ~520 kb MBGC cluster on chromosome 4 of sub-genome C of the allotetraploid *O. alta*
174 (CCDD). This cluster contained orthologs of *MAS*, *KSL4*, *CYP99A2/3*, and three orthologs of
175 *CPS4* (Figure 1b). In contrast, we did not find any orthologs of momilactone biosynthetic genes
176 in the D sub-genome of *O. alta*. This observation is in line with *O. australiensis* (EE), the
177 closest relative of the *O. alta* D-type sub-genome lacking a MBGC (the ancestral diploid D-
178 type donor is presumably extinct) (Bao and Ge, 2004; Ge et al., 1999). In the allotetraploid *O.*
179 *coarctata* (KKLL), we identified a MBGC spanning ~55 kb and containing one ortholog each
180 of *CPS4*, *MAS*, *KSL4*, and *CYP99A2/3*. Based on a species tree obtained from 4,069 multiple-
181 sequence alignments of single-copy orthologs (Figure 1b) and from existing literature (Ge et
182 al., 1999; Guo and Ge, 2005; Shenton et al., 2020), we could tentatively assign the MBGC in
183 *O. coarctata* to chromosome 4 (LG08) of the LL sub-genome (evenly numbered chromosomes
184 in the annotation belong to the LL, unevenly numbered ones to the KK sub-genome). Because
185 this lineage diverged earlier than the MBGC-lacking EE lineage (Figure 1b), we speculate that
186 the cluster most likely became lost in the EE lineage. Lastly, we did not detect the cluster or
187 homologs thereof in *O. granulata* (GG).

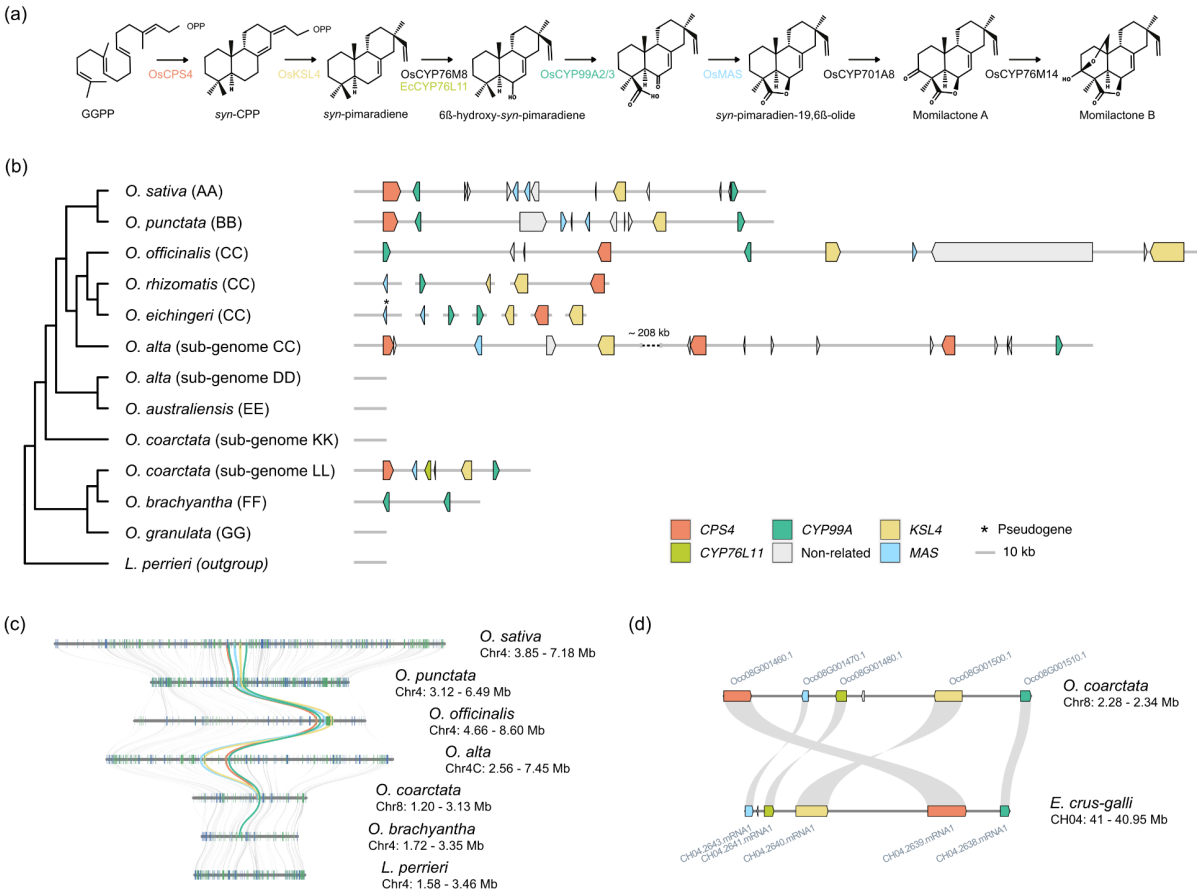

Figure 1. The momilactone biosynthetic gene cluster in the *Oryza* genus. a) Simplified representation of the momilactone biosynthetic pathway, adapted from De la Peña et al. (2021) and Kitaoka et al. (2021). **b)** Phylogenetic relationship between the different *Oryza* species and sub-genomes included in this study, the outgroup *L. perrieri*, and their respective MBGCs. The species tree represents the maximum-likelihood tree inferred from a concatenated multiple-sequence alignment of single-copy orthologs using 4,069 orthogroups with a minimum of 100.0% of species having single-copy genes in any orthogroup. Coloured block arrows represent genes. Scaffold and positional information on all genes is provided in Supplementary Table 2. **c)** Microsynteny between the genomic regions containing the MBGC from *O. sativa*, *O. punctata*, *O. officinalis*, *O. alta*, *O. coarctata*, *O. brachyantha*, and *L. perrieri*. **d)** Microsynteny between MBGC in *O. coarctata* and *E. crus-galli*. Note that this microsynteny does not extend to the flanking regions of the cluster (also see Supplementary Figure 6). In (c) and (d), grey lines connect the respective orthologs. "Non-related" refers to genes that do not seem to be functionally related to the main biosynthetic cascade of the cluster.

To further confirm that we had detected the MBGC and not another diterpene-related BGC, we analysed the synteny of the corresponding regions among the different species. We hypothesized that if the MBGC in the *Oryza* genus had a common origin, one should observe high synteny of the genomic region among all species. We excluded *O. rhizomatis* and *O. eichingeri* from the synteny analysis, because in those genome assemblies the momilactone biosynthesis genes were located on short scaffolds that often carried only very few (~3-4) genes in total. For the remaining species and sub-genomes, the genomic region containing the MBGC (or lacking it, as in the case of *O. alta* sub-genome D, *O. australiensis*, *O. coarctata*

209 sub-genome K, and *O. granulata*) was syntenic (Figure 1c, Supplementary Figure 5). The
210 synteny further confirmed the presence of the MBGC in the different reference genomes and
211 indicated that this region shares a common evolutionary origin. Taken together, these results
212 suggest that the MBGC is prevalent at a basal position of the *Oryza* phylogeny. The evolution
213 of the cluster in different lineages is characterized by differences in cluster size, lineage-
214 specific rearrangements with an important variation in gene copy number, and lineage-specific
215 loss of the cluster.

216 *Species-specific deviations in the MBGC architecture in the Oryza genus*

217 We next investigated whether there were any noticeable species-specific deviations in the
218 MBGC architecture. In *O. coarctata*, we identified an extra gene located between *MAS* and
219 *KSL4* and encoding a CYP. Importantly, this enzyme does not belong to the CYP99A
220 subfamily, which is the canonical CYP in the MBGC of the other *Oryza* species (Figure 1b).
221 Instead, the MBGC in *O. coarctata* strikingly resembled that of *E. crus-galli* (Figure 1d), which
222 also contains an additional CYP-encoding gene, *EcCYP76L11*, that does not belong to the
223 CYP99A subfamily either (Guo et al., 2017; Kitaoka et al., 2021). EcCYP76L11 catalyses the
224 same reaction as OsCYP76M8, converting *syn*-pimaradiene to 6β-hydroxy-*syn*-pimaradiene
225 (Kitaoka et al., 2021). In rice, *OsCYP76M8* is located outside of the MBGC, which suggests
226 that *E. crus-galli* possibly contains a more compacted version of the cluster (Kitaoka et al.,
227 2021).

228 We further investigated the MBGC in *O. coarctata*. An initial microsynteny comparison of the
229 MBGCs in *O. coarctata* and *E. crus-galli* revealed that the additional CYP-encoding gene could
230 indeed be an ortholog of *EcCYP76L11* (Figure 1d). Notably, the microsynteny pattern was
231 restricted to the MBGC itself and not to the flanking regions of the cluster in both species
232 (Supplementary Figure 6). We confirmed that this additional CYP-encoding gene was a
233 reciprocal best hit to EcCYP76L11. To verify the relationship between the CYP-encoding gene
234 in *O. coarctata* MBGC and *EcCYP76L11*, we conducted an amino-acid-sequence-based
235 phylogenetic analysis including all *Oryza* species from our panel and different representative
236 species of the main Poaceae subfamilies (Supplementary Figure 7; see Material and Methods
237 for details). Our analysis placed the *O. coarctata* CYP (Oc08G001480) in a clade with
238 EcCYP76L11 (CH04.2641), the two CYP76L11 paralogs from the MBGC of *E. haploclada*
239 (eh_chr4.2731 and eh_chr4.2733) (Wu et al. 2022) and two CYPs from *P. hallii*
240 (Pahal.1G039100) and *S. italica* (Seita.2G145700), respectively. Interestingly, the *O.*
241 *coarctata* CYP did not group in a clade with the unique CYP76L member from *O. sativa*

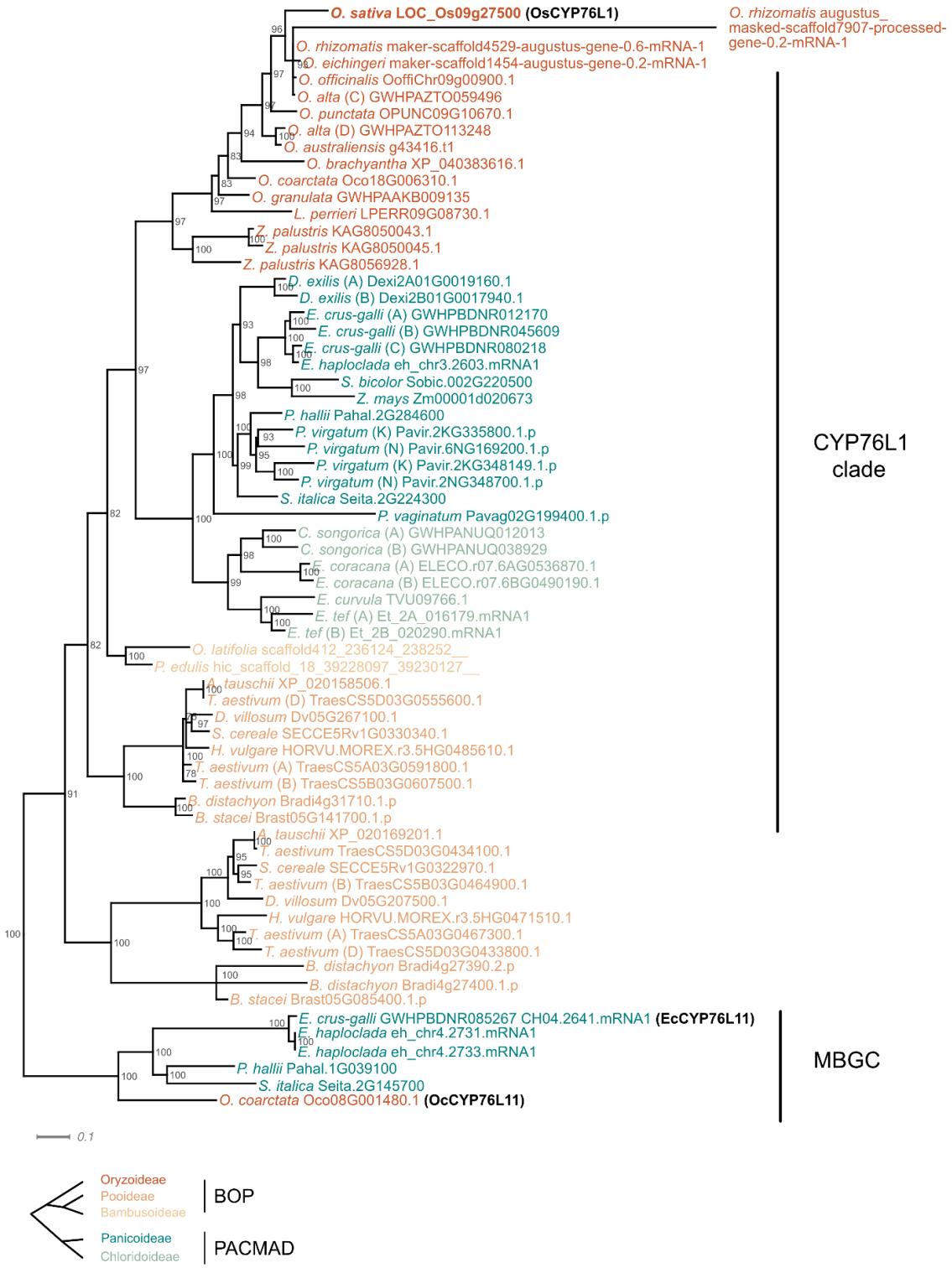

Figure 2. Phylogenetic analysis of a newly identified CYP ortholog in the MBGC. Subtree extracted from the maximum likelihood tree with the best-fit model selected by ModelFinder representing the relationship between the orthogroup containing *O. coarctata* CYP76L11 (see also Supplementary Figure 8). The phylogenetic tree is based on amino acid sequence alignments of the OsCYP76L1 clade, EcCYP76L11 and OcCYP76L11 (both present in the *E. crus-galli* and *O. coarctata* MBGC, respectively), and *Poaceae* species belonging to the subfamilies Oryzoideae, Pooideae, Bambusoideae, Panicoideae and Chloridoideae. The phylogenetic relation between these subfamilies is represented in the bottom graph.

250 (OsCYP76L1) or the CYP76L1 orthologs in other *Oryza* species (including Oc18G006310
251 from *O. coarctata*) (Figure 2). Consequently, based on the similarity to EcCYP76L11, we
252 named the newly identified *O. coarctata* CYP-encoding gene *OcCYP76L11*. Our analysis
253 suggests that *OcCYP76L11* was present in the ancestral *Oryza* MBGC and was retained in
254 the early-divergent *O. coarctata*, while it became lost in the later-diverging clades of the *Oryza*
255 genus.

256 *Momilactone production in different Oryza lineages*

257 Among the investigated *Oryza* genome types (CC, CCDD, EE, KKLL and GG), only species
258 and sub-genomes belonging to the lineages CC and LL include an orthologous MBGC.
259 Notably, *O. coarctata* (KKLL), the earliest-divergent *Oryza* species with a MBGC, showed a
260 distinct cluster architecture. To assess the functionality of the predicted clusters in the CC and
261 LL lineages, we proceeded to evaluate the momilactone-producing potential of their respective
262 representative species *O. officinalis* (CC) and *O. coarctata* (KKLL).

263 We conducted liquid chromatography-tandem mass spectrometry (LC-MS/MS) or ultra-high
264 performance liquid chromatography (UHPLC)-MS/MS to detect momilactones A and B in leaf
265 blades. Momilactone basal levels can be close to detection limits, which is why we induced
266 momilactone production by treating the plants with $CuCl_2$ 3 days before extraction, a treatment
267 previously shown to increase momilactone levels in different *Oryza* species (Miyamoto et al.,
268 2016). Consistent with the presence of the MBGC and the similar expression pattern of the
269 corresponding genes upon induction (Supplementary Figure 9), we detected both
270 momilactone A and B in *O. officinalis* (Figure 3a), but only momilactone A in *O. coarctata*
271 (Figure 3b-e). Even after induction by $CuCl_2$, *O. coarctata* accumulated only low levels of
272 momilactone A (Figure 3b-e). Taken together, these results provide evidence for the
273 functionality of the identified MBGC in the CC and KKLL species *O. officinalis* and *O. coarctata*,
274 respectively.

275 *Functional analysis of KSL4 in O. officinalis and O. coarctata*

276 After establishing the existence of orthologous MBGCs in wild relatives of cultivated rice from
277 the *Oryza* genus and confirming the presence of momilactone A and B in *O. officinalis* and
278 momilactone A in *O. coarctata*, we next wanted to confirm the enzymatic functionality of the
279 orthologs from those clusters. We focused on KSL4, which is known to catalyse the first
280 dedicated step towards momilactone biosynthesis (*i.e.*, the conversion of *syn*-CDP to 9βH-
281 pimara-7,15-diene). We tested the enzymatic activity of the KSL4 orthologs in representative

species of the late-diverged CC and early-diverged KKLL lineages: OoKSL4-1 and OoKSL4-2 from *O. officinalis*, and OcKSL4 from *O. coarctata*.

The available annotation of the genes in the MBGC in *O. officinalis* showed inconsistencies, such as an extra sequence of amino acids in the C-terminal part of OoKSL4-1 and a missing exon in both *OoKSL4-1* and *OoKSL4-2*, compared to the ortholog in *O. sativa* (*OsKSL4*) (Supplementary Figure 10). These discrepancies may be attributed to limitations in the genome annotation process, which relied on RNA-seq data from tissues in which the constitutive expression of momilactone biosynthetic genes is generally low or absent (Supplementary Figure 9) (Shenton et al., 2020).

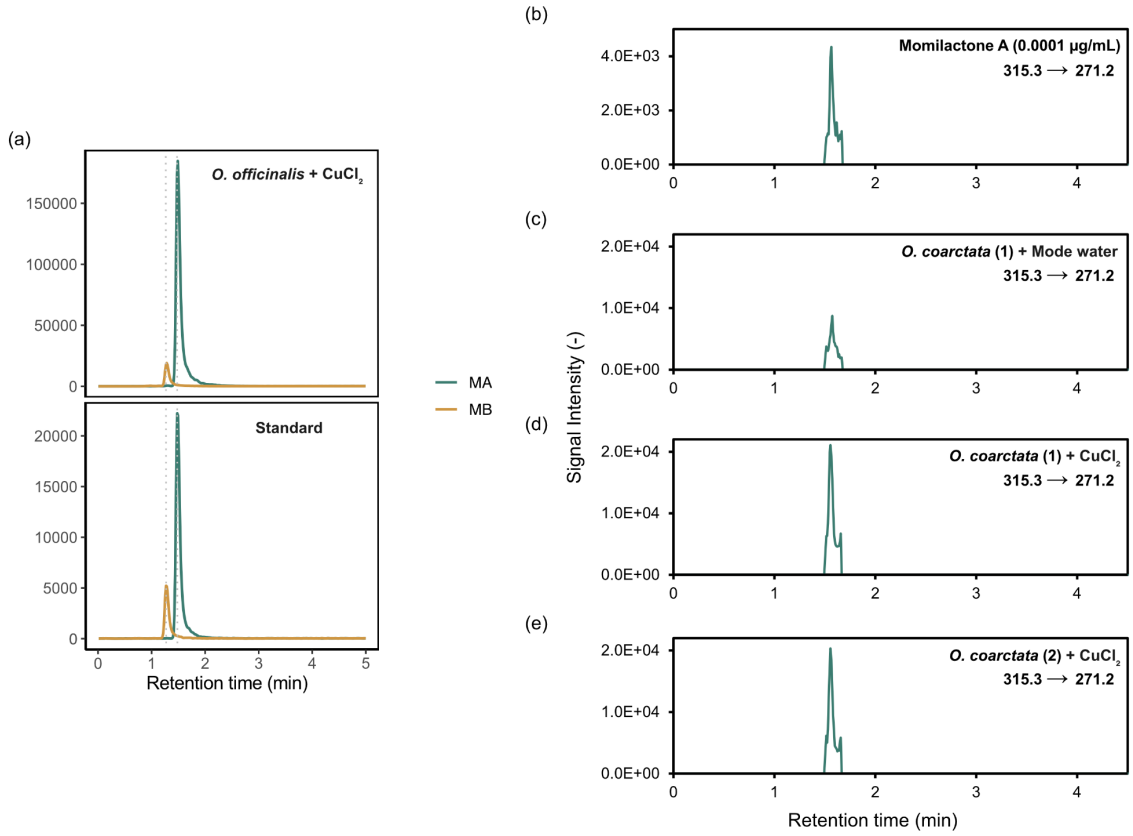

Figure 3. **Analysis of momilactones in representative species of the *Oryza* genus. (a)** Extracts from *O. officinalis* $CuCl_2$-treated leaf blades were analysed by liquid chromatography-tandem mass spectrometry (LC-MS/MS). Five µl of the extract were subjected to LC-MS/MS under the conditions described in the Materials and Methods section. Momilactones were detected with combinations of m/z 315/271 for momilactone A and m/z 331/269 for momilactone B in the multiple reaction monitoring mode. MA, momilactone A; MB, momilactone **(b-e)**. Ultra-high performance liquid chromatography (UHPLC)-MS/MS (ESI^+) chromatograms in the scheduled MRM mode of momilactone A in reference solution (0.0001µg/mL) **(b)**, mode water *O. coarctata* **(c)**, $CuCl_2$-treated leaf blades of *O. coarctata* replicate 1 **(d)** and $CuCl_2$-treated leaf blades of *O. coarctata* replicate 2 **(e)** showing the specific mass transition m/z 315.3 / 271.2 used for quantitation.

301 Exposure to UV light is known to induce the accumulation of momilactones in rice leaves
302 (Kodama et al., 1988). To accurately investigate the function of KSL4 in *O. officinalis* and *O.*
303 *coarctata*, we used previously published mRNA-Seq data from UV-irradiated leaf sheaths of
304 both species to assemble a *de novo* transcriptome (Itoh et al., 2021). Subsequently, we
305 conducted a homology search for OsKSL4 homologs in *O. officinalis* and *O. coarctata*. Using
306 the assembled contig sequences as a reference, we designed specific primers and
307 successfully cloned the cDNAs of these three *KSL4* homologs. We noticed that all cDNA
308 clones of *OoKSL4-2*, obtained from independent plants of the same accession as the
309 reference genome (W0002), exhibited a single nucleotide polymorphism (SNP) at position
310 7,882,960 that resulted in a G-to-A substitution, introducing a premature stop codon at amino
311 acid position 445 (Supplementary Figure 10 and 11). We confirmed that all plants in our study
312 were derived from one specific individual plant from the stock centre, and that this clone carried
313 a *de novo* mutation that had been clonally propagated during plant material distribution; further
314 investigation revealed that this SNP was absent in 14 other *O. officinalis* accessions, including
315 the reference genome sequence of accession W0002, and hence is not representative of the
316 consensus sequence at the population level (Supplementary Figure 11). We therefore
317 reverted the G-to-A polymorphism in our cDNA clone to the consensus reference sequence
318 of *OoKSL4-2*. We proceeded to confirm the enzymatic activity of OoKSL4-1, OoKSL4-2 and
319 OcKSL4 by performing a *syn*-CDP conversion assay in *E. coli* and analysing the products
320 using gas chromatography coupled to mass spectrometry (GC-MS). The retention time of the
321 product generated by OoKSL4-2 and OcKSL4 was identical to that of 9βH-pimara-7,15-diene,
322 indicating that both enzymes have the same enzymatic activity as OsKSL4 (Figure 4a). In
323 contrast, we did not observe any production of 9βH-pimara-7,15-diene by OoKSL4-1, but
324 production of minute amounts of an unidentified product (labelled as “b” in Figure 4a). We
325 were able to corroborate the production of 9βH-pimara-7,15-diene by OoKSL4-2 by transiently
326 expressing OoKSL4-1 and OoKSL4-2 in *Agrobacterium tumefaciens*-infiltrated *Nicotiana*
327 *benthamiana* leaves (Figure 4b). We therefore conclude that OoKSL4-2 is the enzyme
328 responsible for catalysing the conversion of *syn*-CDP to *syn*-pimaradiene in *O. officinalis*.
329 Taken together, these results further support that the orthologous MBGC the we identified in
330 *O. officinalis* and *O. coarctata* are functional and responsible for the production of
331 momilactones.

332

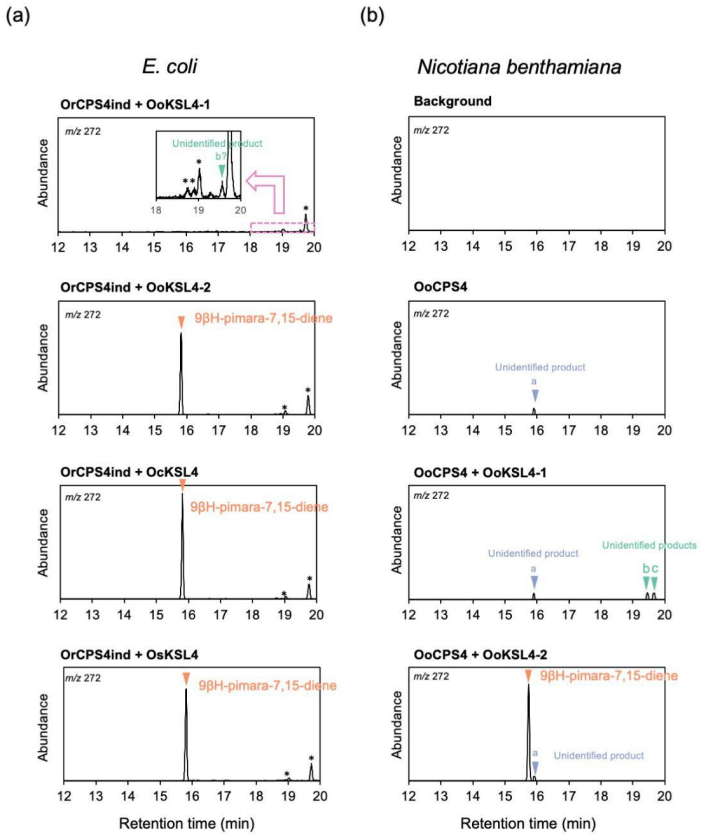

Figure 4. Functional characterization of KSL4 orthologs. a) GC-MS chromatograms of the products obtained from recombinant OoKSL4-1, OoKSL4-2 (with the reverted Trp at position 445), OcKSL4, and OsKSL4 from *E. coli* in a metabolic engineering system. **b)** GC-MS chromatograms of the products obtained in the *Nicotiana benthamiana* transient expression system after expressing *OoCPS4*, *OoCPS4* + *OoKSL4-1* and *OoCPS4* + *OoKSL4-2*. Orange triangles indicate production of 9βH-pimara-7,15-diene. Non-specific peaks from *E. coli* cells are indicated with asterisks (*). Mass spectra are included in Supplementary Figure 12.

DISCUSSION

The momilactone BGC shows diversified architecture within the Oryza genus

BGCs arise from the duplication of enzymes involved in primary metabolism, followed by neofunctionalization and/or relocation processes that are influenced by positive and negative selection pressures (Polturak et al., 2022b; Smit and Lichman, 2022). Ecological factors shape the direction and strength of the selection process, determining the evolution of the metabolism and ultimately affecting the architecture of BGCs. Here, we studied the composition and evolution of the momilactone biosynthetic gene cluster in previously unexplored lineages in the genus *Oryza*. We provide evidence that the MBGC is prevalent in the CC and LL lineages, while it is absent in the intermediate EE or the basal GG lineages (Figure 1b). Our data show that the evolution of the MBGC is marked by lineage-specific rearrangements, such as gene copy number variation or the increase of the size of the cluster,

352 on-going pseudogenization in certain paralogs, and occasional cluster loss. Moreover, we
353 found a distinct MBGC architecture in *O. coarctata*, with the cluster in that species harbouring
354 a close ortholog of *EcCYP76L11*. This finding represents the first instance of an alternative
355 architecture of the MBGC in *Oryza* and strengthens the idea of a common origin of the MBGC
356 in *Echinochloa* and *Oryza*. Overall, our research sheds light on the evolutionary dynamics and
357 distribution of the MBGC in the genus *Oryza*.

358 In our study, we found the MBGC at a basal position of the *Oryza* phylogeny in the species *O.*
359 *coarctata* (sub-genome LL). *O. coarctata* is a polyploid species resulting from the hybridization
360 of the KK and LL diploid genomes; the respective ancestral species have presumably gone
361 extinct or remain to be discovered (Ge et al., 1999; Lu et al., 2009). The KK sub-genome
362 occupies a basal position relative to the EE and DD lineages, while the *O. coarctata* LL sub-
363 genome (initially designated as HH) occupies a more basal position compared to KK and it is
364 closer to the diploid FF genome species *O. brachyantha*. Since we found the cluster in *O.*
365 *coarctata*, a species that branched off before the divergence of the EE lineage, we hypothesize
366 that *O. australiensis* (EE) likely lost the MBGC. Our study thereby is one of the very few to
367 document a case of inter-specific loss of biosynthetic gene clusters (Smit and Lichman, 2022).
368 A lineage-specific loss of a BGC was previously described in *Oryza* for the phytocassane
369 biosynthetic gene cluster: *Oryza* AA species and the outgroup species *L. perrieri* and *Zizania*
370 *palustris* possess the phytocassane cluster, whereas it was partially lost in *O. punctata* (BB)
371 and *O. brachyantha* (FF) (Miyamoto et al., 2016; Yan et al., 2022). It is worth noting that the
372 MBGC is also found in the *Panicoideae* and *Chloridoideae* subfamilies of the *Poaceae* and
373 most likely evolved from a common ancestor (Wu et al., 2022a). However, the distribution of
374 the cluster in the PACMAD clade is restricted to certain tribes, while it is either fragmented or
375 completely lost in others (Wu et al., 2022a). In line with these observations, our results
376 highlight the dynamic nature of biosynthetic gene clusters and suggest that loss of BGCs might
377 be prevalent within *Poaceae*.

378 The MBGC and MBGC-like clusters are widespread in the *Poaceae* family (Wu et al., 2022a).
379 Species belonging to the *Triticeae* tribe (Pooideae), phylogenetically more closely related to
380 *Oryza* than to *Echinochloa*, possess a functionally distinct diterpene cluster that shares
381 similarities with the MBGC (Liu et al., 2021; Polturak et al., 2022a; Wu et al., 2022a). This
382 MBGC-like is located on the homeologous chromosomes 2A and 2D in wheat (*Triticum*
383 *aestivum*), homologs of rice chromosome 4, and exhibits synteny with the region containing
384 the MBGC in rice (Polturak et al., 2022a). However, the cluster in *Triticeae* lacks certain
385 important momilactone biosynthesis genes, e.g. a *MAS* and a *syn-CPS* to produce *syn*

386 labdane-related diterpenoids. Instead, the *Triticeae* cluster produces normal labdane-related
387 diterpenoids in wheat (*Triticum aestivum*) and barley (*Hordeum vulgare*) (Liu et al., 2021;
388 Polturak et al., 2022a). Owing to the shared synteny between the MBGC in rice and the
389 MBGC-like in wheat, Polturak et al. suggested that the *Triticeae* diterpene cluster and the
390 MBGC share a common evolutionary origin, and hypothesized that both clusters could have
391 originated from a common ancestral BGC before the divergence of the PACMAD and BOP
392 clades (Polturak et al., 2022a). Wu and colleagues, who performed a more extensive survey
393 of the MBGC in different Poaceae genomes, alternatively attributed the evolution of the cluster
394 in Poaceae to multiple instances of lateral gene transfer (LGT) and proposed that the MBGCs
395 found in the PACMAD clade (Panicoideae and Chloridoideae subfamilies) originated from the
396 MBGC-like cluster in *Triticeae* (Wu et al., 2022a). They moreover speculated that
397 *EcCYP76L11* in *Echinochloa* was also laterally transferred from the *Triticeae* clade along with
398 the MBGC-like. After the PACMAD species acquired the MBGC-like, it would then have
399 recruited *MAS*. Subsequently, another LGT event would have had to occur, resulting in the
400 acquisition of the cluster by *Oryzoideae*, followed by the loss of the *CYP76L11* gene (Wu et
401 al., 2022a). Wu and colleagues based their conclusions on the phylogenetic incongruences
402 among the MBGC orthologous genes, topology tests on the constrained trees for each MBGC
403 gene, and a general lack of synteny between the genomic region containing the MBGC in the
404 different tribes in the *Poaceae*. It is worth noting that the MBGC in *Panicoideae* and
405 *Chloridoideae* is also not syntenic, following the same reasoning, this would imply that these
406 gene clusters were acquired through two separate and independent lateral gene transfer
407 (LGT) events rather than evolving from a common ancestor, as suggested by the same
408 authors. There are several phylogenomic studies that suggest that LGT is prevalent among
409 grasses; LGTs in *Poaceae* usually occur among closely related species, while the insertion
410 occurs in random and non-syntenic genomic regions; however, the underlying mechanisms
411 by which natural plant-plant LGT would occur are still largely unknown (Dunning et al., 2019;
412 Hibdige et al., 2021). Our findings provide evidence that the *CYP76L11* gene has not been
413 completely lost in the genus *Oryza*. The discovery of *CYP76L11* in *O. coarctata* implies either
414 a common origin by vertical transmission of the MBGC between *Echinochloa* and *Oryza*, or a
415 lateral gene transfer (LGT), as proposed by Wu et al. (2022). However, the findings from both
416 Polturak et al. (2022a) and our study (Supplementary Figure 13) indicate high synteny
417 between the flanking regions containing the MBGC-like cluster in *Triticeae* and the MBGC in
418 *Oryza* (including *O. coarctata*) and thus suggest a common evolutionary origin of this genomic
419 region, including the MBGC. This suggests that there may have been a common ancestor of

420 the MBGC that existed before *Oryza* and *Triticeae* diverged. However, it is difficult to reconcile
421 the synteny results shown by us and Polturak *et al*. (2022a) with the phylogenomic signatures
422 of LGT shown by Wu et al., especially considering that the MBGC in *Echinochloa* and *Oryza*
423 produces the same type of compounds, unlike in *Triticeae*. To shed light onto this question, it
424 is important to consider the impact and prevalence of gene and MBGC losses in *Poaceae*.
425 The presence or absence of MBGCs in different species can have significant implications for
426 phylogenomic signals and evolutionary dynamics. The loss of MBGCs in certain lineages
427 could potentially shape the phylogenomic patterns observed in Poaceae. Further
428 investigations into the frequency and significance of MBGC losses across Poaceae will
429 contribute to a better understanding of the evolutionary history of this cluster.

430 *Allotetraploid rice species carry only one MBGC copy in their genome*

431 In our study, we aimed to investigate whether allotetraploid species retain two copies of the
432 MBGC. Previous research has shown that whole genome duplication (WGD) can lead to the
433 silencing and progressive loss of one copy of a biosynthetic gene cluster, likely to balance the
434 effects of increased gene dosage (Polturak et al., 2022a; Yang et al., 2021). We found that
435 each of the two allotetraploid species we studied had retained one copy of the MBGC. In *Oryza*
436 *alta* (CCDD), the cluster was present in the CC but not the DD sub-genome, which means that
437 the MBGC was either lost in the DD sub-genome after hybridization or that the DD ancestor
438 had already lost it prior to the hybridisation. Given that *O. australiensis* (EE), the closest
439 relative of the *O. alta* D-type sub-genome (the ancestral diploid D-type donor is presumably
440 extinct), lacks a MBGC, it is possible that the cluster had already been lost in the DD donor.

441 Similarly, we identified only one copy of the MBGC in the *O. coarctata* LL but not the KK sub-
442 genome. The LL sub-genome derives from a donor species that diverged earlier than the KK
443 sub-genome and is more closely related to *O. brachyantha* (FF), a species that harbours an
444 incomplete MBGC (Guo and Ge, 2005; Miyamoto et al., 2016). However, we cannot say with
445 certainty whether the cluster was lost in the KK sub-genome after hybridization or was already
446 lost prior to the hybridisation in the ancestor. Future studies using yet-to-be generated
447 haplotype-resolved assemblies of BBCC hybrid species could contribute to a better
448 understanding of cluster evolution in allotetraploid rice, as both ancestors of these hybrids
449 harbour the MBGC.

450 *Momilactone B formation may be a recent innovation in the Oryza genus*

451 At the interspecies level, the existence of conserved BGCs does not always align consistently
452 with the production of identical metabolites, while the metabolites derived from orthologous

453 BGCs can also be species-specific. The resulting divergence in chemotypes between species
454 is associated with variations in biosynthetic genes external to the BGC, genes within the BGC,
455 or transcription factors controlling the biosynthesis of these compounds (Liu et al., 2020; Zhou
456 et al., 2016). In some cases, the function of the BGC is retained, and orthologous BGCs
457 produce the same molecule. This is exemplified by *Oryza* species from the AA and BB
458 lineages, which produce momilactones A and B (Miyamoto et al., 2016).

459 In our study, we show that the function of the MBGC is not only retained in the AA and BB but
460 also the CC and LL lineages. Specifically, we found that the CC lineage, represented by *O.*
461 *officinalis*, possesses an MBGC with slight differences in gene copy number, and that both
462 momilactone A and B can be detected. The KKLL species *O. coarctata* contains an
463 orthologous and syntenic MBGC with a distinct architecture compared to *O. sativa*. In line with
464 our phylogenomic analysis suggesting the potential for momilactone production in *O. coarctata*
465 and the co-expression of its MBGC genes, we were able to detect momilactone A in leaf blades
466 induced with $CuCl_2$ (Miyamoto et al., 2016). However, we did not detect momilactone B in *O.*
467 *coarctata*. Among the auxiliary genes outside the MBGC, *CYP701A8* and *CYP76M8* are
468 necessary for the production of momilactone A, while CYP76M14 catalyses the conversion of
469 momilactone A to momilactone B (Figure 1a) (De La Peña and Sattely, 2021; Kitaoka et al.,
470 2021). The lack of momilactone B in *O. coarctata* could be attributed to the suppressed
471 expression of the *CYP76M14* ortholog (*Oc01G012750*), which was only weakly expressed (<3
472 TPM) upon UV treatment and barely detectable under control conditions in different tissues
473 (Supplementary Figure 9). Intriguingly, unlike the MBGC genes, which are located on the LL
474 sub-genome in *O. coarctata*, the only copy of *OcCYP76M14* is located on the KK sub-genome.
475 To date, among the Poaceae, momilactone B has been detected only in AA, BB (Miyamoto et
476 al. 2016) and CC *Oryza* species (this study). At a larger phylogenetic scale, *CYP76M14* is
477 exclusive to *Oryza*, specifically to AA, BB, CC and KK lineages, and appears to have arisen
478 from a duplication within the CYP76M subfamily (Supplementary Figure 8). It is imaginable
479 that the production of momilactone B might have evolved after the divergence of the KK
480 lineage by recruiting *CYP76M14* into the momilactone regulatory network.

481 MATERIALS AND METHODS

482 *Oryza and Poaceae datasets*

483 *O. sativa* (v7.0) (Ouyang et al., 2007) protein sequences and gene annotations were
484 downloaded from Phytozome (https://phytozome-next.jgi.doe.gov/); *O. punctata*

485 (Oryza_punctata_v1.2) (Stein et al., 2018) protein sequences and gene annotations from
486 EnsemblPlants; the *O. officinalis* (Shenton et al., 2020) genome sequence from NCBI
487 (assembly GCA_008326285.1) and annotations from the original article repository; *O.*
488 *eichingeri* and *O. rhizomatis* (Shenton et al., 2020) protein sequences and gene annotations
489 from Cyverse Data Commons (https://doi.org/10.25739/awh3-dm39); *O. alta* (Yu et al., 2021)
490 protein sequences and gene annotations from the from the Genome Warehouse (GWH)
491 accession number GWHAZTO00000000; the *O. australiensis* (Phillips et al., 2022) genome
492 sequence from the National Center for Biotechnology Information (NCBI) (GCA_019925245.2)
493 and annotations from figShare
494 (https://figshare.com/collections/Oryza_australiensis_Keep_River_Genome_Assembly_V2/5
495 875592/2); the *O. coarctata* (Zhao et al., 2023) protein sequences and gene annotation from
496 figShare (https://figshare.com/articles/dataset/A_high-quality_chromosome-
497 level_wild_rice_genome_of_i_Oryza_coarctata_i_/23938590/1); the *O. brachyantha* (Chen et
498 al., 2013) (ObraRS2) genome assembly and gene annotations from NCBI
499 (GCF_000231095.2); *O. granulata* (Shi et al., 2020) protein sequences and gene annotations
500 from GWH (GWHAAKB00000000); *L. perrieri* (Stein et al., 2018) protein sequences and gene
501 annotations (V1.4) from EnsemblPlants*. O. officinalis*, *O. australiensis* and *O. brachyantha*
502 protein sequences were extracted from the gene annotation using gffread (v0.12.7) (Pertea
503 and Pertea, 2020).

504 *Aegilops tauschii subsp. strangulata* (V5.0; GCF_002575655.2) (Wang et al., 2021) protein
505 sequences were retrieved from NCBI, *Brachypodium stacei* (v1.1) (Gordon et al., 2020) from
506 Phytozome, *Brachypodium distachyon* (V3.1) (Sreedasyam et al., 2023; Vogel et al., 2010)
507 from Phytozome; *Cleistogenes songorica* (Zhang et al., 2021) from GWH accession
508 PRJCA002752; *Digitaria exilis* (CM05836) (Abrouk et al., 2020) from article repository in
509 Dryad; *Eleusine coracana* (v1.1) (Devos et al., 2023) from Phytozome; *Echinochloa crus-galli*
510 (V3.0) (Wu et al., 2022b) sequences from GWH, accession number GWHBDNR00000000;
511 Echinochloa haploclada from (Ye et al., 2020) article repository; *Eragrostis curvula*
512 (CERZOS_EC1.0; GCA_007726485.1) (Carballo et al., 2019) from NCBI; *Eragrostis tef*
513 (ASM97063v1) (Cannarozzi et al., 2014) from Ensembl Plants; *Hordeum vulgare* cv Morex
514 (V3) (Mascher et al., 2021) sequences from e!DAL (DOI: 10.5447/ipk/2021/3), we specifically
515 used the file Hv_Morex.pgsb.Jul2020.aa.fa that includes low confidence proteins. Unlike in
516 databases such as Phytozome and EnsemblPlants, this annotation includes most of the gene
517 in the diterpene cluster reported by (Liu et al., 2021); *Olyra latifolia* (Guo et al., 2019)
518 sequences from http://www.genobank.org/bamboo; *Oropetium thomaeum* (v1.0) (VanBuren

519 et al., 2015) from Phytozome; *Phyllostachys edulis* (Zhao et al., 2018) from
520 http://gigadb.org/dataset/100498; *Panicum hallii* var. *filipes* (V3.2) (Lovell et al., 2018)
521 sequences from Phytozome; *Panicum virgatum* (v5.1) (Lovell et al., 2021; Sreedasyam et al.,
522 2023) from Phytozome; *Paspalum vaginatum* (v3.1) (Sun et al., 2022) from Phytozome;
523 *Pharus latifolius* (Ma et al., 2021) sequences from http://www.genobank.org/grass; *Sorghum*
524 *bicolor* (V3.1.1) (McCormick et al., 2018) from Phytozome, *Secale cereale*
525 (Lo7_2018v1p1p1.pgsb.Feb2019.HC) (Rabanus-Wallace et al., 2021) from article repository;
526 *Setaria italica* (V2.2) (Bennetzen et al., 2012) sequences from Phytozome; *Triticum aestivum*
527 cv Chinese Spring (IWGSC V2.1) (Zhu et al., 2021) from
528 https://urgi.versailles.inrae.fr/download/iwgsc/IWGSC_RefSeq_Annotations/v2.1/ (file
529 iwgsc_refseqv2.1_annotation_200916_HC_pep.valid), *Zea mays* B73 (Schnable et al., 2009)
530 (V4) from Phytozome and *Zizania palustris* (Haas et al., 2021) from NCBI (accession
531 JAAALK000000000) and *Ananas comosus* (V3) (Ming et al., 2015) proteome from Phytozome
532 as outgroup.

533 *MBGC ortholog detection*

534 OrthoFinder (v2.5.4) (Emms and Kelly, 2019, 2015) was used to infer orthogroups containing
535 *O. sativa* momilactone biosynthesis genes (i.e., genes from multiple species descended from
536 a single gene in the last common ancestor of these species). In the case of the *Oryza* dataset,
537 the input for OrthoFinder included primary transcript proteomes of the following species: *O.*
538 *sativa*, *O. punctata*, *O. officinalis*, *O. eichingeri*, *O. rhizomatis*, *O. alta*, *O. australiensis*, *O.*
539 *coarctata*, *O. brachyantha*, *O. granulata*, and *L. perrieri* (included as the out-group). We used
540 the '-M msa' option to also infer the species tree (described in Emms and Kelly, 2018). Briefly,
541 a maximum-likelihood species tree was inferred by using concatenated multiple sequence
542 alignment of single-copy orthologs using 4069 orthogroups with a minimum of 100.0% of
543 species having single-copy genes in any orthogroup.

544 Each orthogroup was aligned using MAFFT (v7.490) (Katoh et al., 2002; Katoh and Standley,
545 2013). IQTREE (v2.1.4-beta) (Minh et al., 2020) was used to infer the maximum likelihood
546 (ML) tree with the best-fit model selected by ModelFinder (Kalyaanamoorthy et al., 2017) with
547 1000 replicates of ultrafast bootstrapping (Hoang et al., 2018).

548 ML rooted trees of each orthogroup were used to identify orthologs of *O. sativa* momilactone
549 biosynthetic genes in *Oryza*. Genes within the same clade as *O. sativa* momilactone
550 biosynthesis genes were considered as potentially clustered homologs. The genomic location

551 upstream and downstream of these homologs was further analyzed to confirm clustering.
552 Trees were represented with Dendroscope (v3.8.2).

553 As a quality control measure to ensure no potential momilactone genes were missed, we
554 performed nBLAST using the genomic locus of each momilactone gene from *O. sativa* against
555 each of the *Oryza* species studied. Where necessary, we manually annotated the given locus
556 (i. e. *OoCYP76M14*).

557 *Oryza coarctata CYP76L11 orthologs*

558 To infer the relationship between *EcCYP76L11 and OcoCYP76L11*, we used OrthoFinder to
559 infer the orthogroup containing OcoCYP76L11. The input for OrthoFinder included the primary
560 transcript proteomes of the *Oryza* species described previously, together with *Z. palustris*
561 (Oryzoideae), *T. aestivum*, *A. tauschii*, *S. cereale*, *D. villosum*, *H. vulgare*, *B. distachyon*, *B.*
562 *stacei* (Pooideae); *P. edulis*, *O. latifolia* (Bambusoideae); *Z. mays*, *S. bicolor*, *P. vaginatum*,
563 *E. crus-galli*, *E. haploclada*, *S. italica*, *P. hallii*, *P. virgatum*, *D. exilis* (Panicoideae); *E.*
564 *coracana*, *C. songorica*, *O. thomaeum*, *E. curvula*, *E. tef* (Chloridoideae); *P. latifolius*, as
565 outgroup to the core Poaceae; and *A. comosus* as outgroup of Poaceae.

566 The orthogroup containing OcoCYP76L11 was aligned using MAFFT (v7.490) followed by the
567 inference of the maximum likelihood (ML) tree with IQTREE (v2.1.4-beta) and selecting the
568 best-fit model by ModelFinder with 1000 replicates of ultrafast bootstrapping.

569 *Microsynteny Analysis*

570 Microsynteny analysis and figures were done with MCScan implemented in Python (v3.9) with
571 JCVI utility libraries (v1.1.11) following the package workflow:
572 https://github.com/tanghaibao/jcvi/wiki/MCscan-(Python-version). Scripts are detailed in
573 https://github.com/spriego/Priego-Cubero-et-al.-Oryza. Briefly, protein FASTA files and GFF3
574 files of each species were used as input. When needed, the FASTA files
575 were processed using Biopython's SeqIO package (Cock et al., 2009). Pairwise ortholog and
576 synteny blocks search was performed with default settings using a lift-over distance of 5, a c-
577 score = 0.99 and a maximum of 1 iterations. Multi-synteny blocks were constructed combining
578 the syntenic blocks detected on every species with respect to *Oryza sativa*.

579 *RNA-seq* mapping and quantification

580 Publicly available RNA-seq datasets from *O. officinalis* and *O. coarctata* were used (see
581 Supplementary Figure 9). RNA-seq mapping and quantification was done using the nf-core

582 pipeline rnaseq v3.14 (https://nf-co.re/rnaseq/3.14.0) in Nextflow 22.10.4 (Patel et al., 2024).
583 Briefly, adapter and quality trimming was performed using TrimGalore v0.6.7 (Krueger et al.,
584 2021). Then, reads were mapped to reference genomes using STAR v2.7.9a (Dobin et al.,
585 2013) and quantified using salmon v1.10.1 (Patro et al., 2017). Finally, feature counts were
586 normalised by gene length and sequencing depth using transcripts per million (TPM), that
587 were used to inspect the expression of the momilactones biosynthetic genes.

588 *SNP calling*

589 Short-read Illumina sequencing data for 15 *O. officinalis* accession were downloaded from
590 OryzaGenome 2.1 (http://viewer.shigen.info/oryzagenome21detail/index.xhtml) (Kajiya-
591 Kanegae et al., 2021). SNP calling was performed using the nf-core pipeline sarek v3.0.1 with
592 default parameters in Nextflow 22.10.4 (Cannarozzi et al., 2014; Ewels et al., 2020; Garcia et
593 al., 2020). Briefly, the fastq files underwent sequence quality assessment and pre-processing
594 using fastp v0.23.2 (Chen et al., 2018). The reads were mapped to the *O. officinalis* reference
595 genome using BWA mem v0.7.17-r1188 (Katoh and Standley, 2013). Duplicates were marked
596 with GATK MarkDuplicates version 4.2.6.1 (McKenna et al., 2010). Variant calling was
597 performed with HaplotypeCaller (Poplin et al., 2018). The BaseRecalibrator step was skipped
598 as it requires a database of known polymorphic sites, which is unavailable for *O. officinalis.*
599 The output vcf files were merged with bcftools v1.13 (Danecek et al., 2021) and SNPs effect
600 were annotated with snpEff v5.0.1 (Cingolani et al., 2012).

601 *Data analysis*

602 RStudio with R version 4.3.1 was used for generating Figures 1b, 3a, and Supplementary
603 figures 9 and 11. Scripts used for data analysis are available at
604 https://github.com/spriego/Priego-Cubero-et-al.-Oryza. To generate the figures, the following
605 R packages were used: Tidyverse (Wickham et al., 2019), khroma (Frerebeau, 2023), ggrepel
606 https://github.com/slowkow/ggrepel, readxl https://github.com/tidyverse/readxl, MetBrewer
607 (https://github.com/BlakeRMills/MetBrewer), and MoMAColors
608 (https://github.com/BlakeRMills/MoMAColors).

609 *Plant materials*

610 Seeds of *O. officinalis* (accession W0002) and *O. coarctata* (accession W0551), and genome
611 DNA solutions of several accession of *O. officinalis* (W0002, W0566, 0614, W1131, W1200
612 and W1252) were provided by the Resource Bank of the National Institute of Genetics, Japan
613 (http://www.shigen.nig.ac.jp/rice/oryzabase/locale/change).

614 *Momilactone measurements*

615 Each harvested leaf blade was treated with 0.5 mM $CuCl_2$ for 72 h before the analysis. The
616 treated sample (roughly 100 to 500 mg) was submerged in 4 ml of 70% methanol at 4°C for
617 24 h.

618 For *O. officinalis*, 2 uL of the extract was subjected to LC-MS/MS analysis (Sciex QTRAP3200)
619 with the following selected reaction monitoring transitions used as previously described
620 (Miyamoto et al., 2016): momilactone A, m/z 315/271; momilactone B, m/z 331/269.

621 For *O. coarctata*, plant material (100-150 mg) was weighed in a 2 mL extraction tube (CKMix,
622 Bertin Technologies, Montigny le Bretonneux, France), and the tube filled up with
623 methanol/water (70/30, v/v, 2 mL). After extractive grinding (3 × 30 s with 30 s breaks, 6000
624 rpm) using the bead beater (Precellys Homogenizer, Bertin Technologies, Montigny le
625 Bretonneux, France), samples were incubated for 24 h at 4°C. After centrifugation, the
626 supernatant was evaporated to dryness, resumed in acetonitrile (50 µL), and injected into the
627 UHPLC−MS/MS-system (5 µL).

628 A QTRAP 6500+ mass spectrometer (Sciex, Darmstadt, Germany) was used to acquire mass
629 spectra and product ion spectra in positive electrospray ionization (ESI) mode. The MS/MS
630 system was operated in the scheduled multiple reaction monitoring (MRM) mode at an ion
631 spray voltage of 5500 V with the following ion source parameters: curtain gas (35 psi),
632 temperature (550°C), gas 1 (55 psi), gas 2 (65 psi), and entrance potential (10 V). For analysis
633 of momilactones A and B, the MS/MS parameters were tuned to achieve fragmentation of the
634 [M+H]+ molecular ions into specific product ions: [M+H]+: momilactone A m/z 315.2/271.2
635 (quantifier) and m/z 315.2/269.2 (qualifier), momilactone B m/z 331.3/269.2 (quantifier) and
636 m/z 331.2/128.1 (qualifier). For tuning, acetonitrile/water solutions of each analyte were
637 introduced by means of flow injection using a syringe pump. The samples were separated by
638 means of an ExionLC UHPLC (Shimadzu Europa GmbH, Duisburg, Germany) consisting of
639 two LC pump systems ExionLC AD, an ExionLC degasser, an ExionLC AD autosampler, an
640 ExionLC AC column oven and an ExionLC controller, and equipped with a BEH Premier C18
641 column (150 × 2.1 mm, 100 Å, 1.7 µm, Waters, Manchester, UK). Operated with a flow rate of
642 0.5 mL/min at a column oven temperature of 45°C using 0.1% formic acid in water (v/v) as
643 solvent A and 0.1% formic acid in acetonitrile (v/v) as solvent B. Chromatography was
644 performed with the following gradient: 70% B increased to 77.5% in 2.5 min, increased to
645 100% B in 0.5 min, held 1 min at 100% B, decreased to 70% B in 0.5 min, and held 0.5 min at

646 70% B. Data acquisition, and instrumental control was performed with Analyst 1.6.3 software
647 (Sciex, Darmstadt, Germany).

648 *cDNA cloning of OoKSL4 and OcKSL4 and their functional analysis by metabolic*
649 *engineering systems*

650 The nucleotide sequences of full-length *OoKSL4-1*, *OoKSL4-2* and *OcKSL4* have been
651 deposited in the GenBank database with accession numbers LC831403, LC831404 and
652 LC831406, respectively.

653 For *OoCPS4*, full length of cDNA was amplified by RT-PCR using cDNA prepared from RNA
654 sample of *O. officinalis* leaf 24-hour after the $CuCl_2$ treatment with forward primer (OoCPS4F:
655 5'- TTCTGCCCAAATTCGATGCCGGCCTTTACTGCATC-3'), reverse primer (OoCPS4R: 5'-
656 GTGATGGTGATGCCCAATCACATCTTGGAATATGA-3'). Nucleotide sequence of OoCPS4
657 has been deposited in the GenBank database with accession number LC831405. For
658 *OoKSL4-1* full length cDNA were amplified by RT-PCR using forward primer (OoKSL4-1F: 5'-
659 TTCTGCCCAAATTCGATGGTTATCACCCATATTTTGAG-3'), reverse primer (OoKSL4-1R:
660 5'- GTGATGGTGATGCCCAGATGAACTTGTAGCACCTAG-3'). To recover the nonsense G-
661 to-A polymorphism in *OoKSL4-2*, a 2-step overlap PCR was performed. For the first amplicon,
662 forward primer-1 (OoKSL4-2F1: 5'-TTCTGCCCAAATTCGATGGCGAATCCTATGG-3') and
663 reverse primer-1 (OoKSL4-2R1: 5'-GCTACCTGACCAACAACCCATTT-3') were used. For the
664 second amplicon, forward primer-2 (OoKSL4-2F2: 5'-AAATGGGTTGTTGGTCAGGTAGC-3')
665 and reverse primer-2 (OoKSL4-2R2: 5'-GTGATGGTGATGCCCGTAGCCTATAGTTTTCAG-
666 3') were used. The full length of the recovered *OoKSL4-2* was then amplified using forward
667 primer-1 and reverse primer-2 as the primer set, with amplicons from part 1 and part 2 serving
668 as templates. For *OsDXS3* full length cDNA were amplified by RT-PCR using forward primer
669 (DXS3F: 5'- TTCTGCCCAAATTCGATGGCGCTCCAGGCATCG-3'), reverse primer (DXS3R:
670 5'- GATGCATACCGGTCGTCAGCTGAGCTGAAGTGC-3'). For *OsGGPPS* full length cDNA
671 were amplified by RT-PCR using forward primer (GGPSF: 5'-
672 TTCTGCCCAAATTCGATGGCTGCCTTCCCCCCG-3'), reverse primer (GGPSR: 5'-
673 GATGCATACCGGTCGTCAGTTCTGCCGATAGGC-3').

674 Full length cDNAs of *OoCPS4*, *OoKSL4-1* and *OoKSL4-2*, containing transit peptides, and
675 two genes from *O. sativa* encoding OsDXS3 and OsGGPPS in the MEP pathway were
676 respectively cloned into NruI-SmaI sites of pEAQ-HT vector by In-Fusion cloning system
677 (Takarabio-Clontech). Constructed pEAQ-HT-*OoffKSL4-1*, pEAQ-HT-*OoffKSL4-2*, pEAQ-HT-

678 *OsDXS3* and pEAQ-HT-*OsGGPPS*, all with 6×His tags at the C-terminal region, were then
679 transferred into *Agrobacterium tumefaciens* for agroinfiltration.

680 In the *Nicotiana benthamiana* transient expression system, 5-week-old plants grown in a plant
681 incubator (23°C, 16 h light/8 h dark photoperiod) were used. After agroinfiltration, the plants
682 were further grown for five days under the same conditions. The leaves were then harvested,
683 cut into 5 mm squares, immersed in *n*-hexane for a one-day extraction. Extraction and
684 purification were done as described previously (Toyomasu et al., 2018).

685 The cDNA encoding partial OoKSL4-1 for functional analyses using *E. coli* was amplified by
686 RT-PCR using primers 5'-GGATCCATGGCGAATCCTGTGGAAG-3' (forward; BamHI site is
687 underlined) and 5'-GTCGACTTAAGATGAACTTGTAGCACCTAG-3' (reverse; SalI site is
688 underlined), and subcloned into pGEX-4T-3 (GE Healthcare) using BamHI and SalI. The
689 cDNA encoding pseudo-mature OoKSL4-2 was amplified by RT-PCR using forward primer 5'-
690 GGTTCCGCGTGGATCCGAGGCTAGAATAAGGAGGC-3' and reverse primer 5'-
691 GGGAATTCGGGGATCCCTAGTAGCCTATAGTTTTC-3' (terminal sequences of pGEX-4T-3
692 digested by BamHI are underlined), and inserted into BamHI-digested pGEX-4T-3 by using
693 In-Fusion Smart Assembly Cloning Kit (Takarabio-Clontech). Full-length *OcKSL4* cDNA was
694 amplified by RT-PCR using primers 5'-GGATCCATGGCGAATTATCCCATGGAG-3' (forward;
695 BamHI site is underlined) and 5'-TTAAGATGGACTAGTAGCCTCTAGTTTAAGTGGC-3'
696 (reverse; NotI site is underlined), and subcloned into pGEM-T-Easy. *OcKSL4* cDNA was
697 inserted into pGEX-4T-3 using BamHI and NotI. For RT-PCR, we used cDNA prepared from
698 RNA from leaf blades of *O. officinalis* W0002 and *O. coarctata* W0551 24 h after UV treatment.
699 OoKSL4-2_445W was generated by mutagenesis PCR using OoKSL4-2 in pGEX as template,
700 with primers 5'-gTCAGGTAGCTTATTGAAAC-3' (forward) and 5'-
701 caACAACCCATTTTCTCTAGGATTG-3' (reverse; small characters indicate W codon for
702 mutagenesis).

703 The functional analyses of OoKSL4-1, OoKSL4-2 and OcKSL4 in a metabolic engineering
704 system using *E. coli* cells were performed as described previously (Toyomasu et al., 2016).
705 The *n*-hexane extract from culture medium containing recombinant *E. coli* BL21-DE3
706 harbouring pRSF-PaGGS:OrCPS4ind and a respective construct to express one of the above
707 proteins was subjected to GC-MS analysis. PaGGS is a geranylgeranyl synthase domain of
708 fusicoccadiene synthase in *Phomopsis amygdali* (PaFS) (Toyomasu et al., 2007) and
709 OrCPS4ind is a *syn*-CDP synthase from *O. rufipogon* W0106 (Miyamoto et al., 2016), to
710 supply GGDP and *syn*-CDP, respectively.

711 GC-MS was conducted using an Agilent 8860 GC-5977 MSD system, fitted with a fused silica,
712 chemically bonded capillary column (HP-1MS; 0.25 mm in diameter, 60 m long, 0.25 μm film
713 thickness). Ionization voltage was 70 eV. Each sample was injected onto the column at 250°C
714 in the splitless mode. After a 2-min isothermal hold at 60℃, the column temperature was
715 increased by 30℃/min to 150℃, 10℃/min to 180℃, 2℃/min to 210℃, and 30℃/min to 300℃.
716 The flow rate of the helium carrier gas was 1 mL/min. We used 9βH-pimara-7,15-diene as a
717 standard, which was synthesized as previously described (Ye et al., 2017).

718 REFERENCES

719 Abrouk, M., Ahmed, H.I., Cubry, P., Šimoníková, D., Cauet, S., Pailles, Y., Bettgenhaeuser, J., Gapa,
720 L., Scarcelli, N., Couderc, M., Zekraoui, L., Kathiresan, N., Čížková, J., Hřibová, E., Doležel, J.,
721 Arribat, S., Bergès, H., Wieringa, J.J., Gueye, M., Kane, N.A., Leclerc, C., Causse, S.,
722 Vancoppenolle, S., Billot, C., Wicker, T., Vigouroux, Y., Barnaud, A., Krattinger, S.G., 2020. Fonio
723 millet genome unlocks African orphan crop diversity for agriculture in a changing climate. Nat.
724 Commun. 11, 4488. https://doi.org/10.1038/s41467-020-18329-4
725 Ahuja, I., Kissen, R., Bones, A.M., 2012. Phytoalexins in defense against pathogens. Trends Plant Sci.
726 17, 73–90. https://doi.org/10.1016/j.tplants.2011.11.002
727 Bao, Y., Ge, S., 2004. Origin and phylogeny of Oryza species with the CD genome based on multiple-
728 gene sequence data. Plant Syst. Evol. 249, 55–66. https://doi.org/10.1007/s00606-004-0173-8
729 Bennetzen, J.L., Schmutz, J., Wang, H., Percifield, R., Hawkins, J., Pontaroli, A.C., Estep, M., Feng, L.,
730 Vaughn, J.N., Grimwood, J., Jenkins, J., Barry, K., Lindquist, E., Hellsten, U., Deshpande, S.,
731 Wang, X., Wu, X., Mitros, T., Triplett, J., Yang, X., Ye, C.-Y., Mauro-Herrera, M., Wang, L., Li, P.,
732 Sharma, M., Sharma, R., Ronald, P.C., Panaud, O., Kellogg, E.A., Brutnell, T.P., Doust, A.N.,
733 Tuskan, G.A., Rokhsar, D., Devos, K.M., 2012. Reference genome sequence of the model plant
734 Setaria. Nat. Biotechnol. 30, 555–561. https://doi.org/10.1038/nbt.2196
735 Cannarozzi, G., Plaza-Wüthrich, S., Esfeld, K., Larti, S., Wilson, Y.S., Girma, D., de Castro, E.,
736 Chanyalew, S., Blösch, R., Farinelli, L., Lyons, E., Schneider, M., Falquet, L., Kuhlemeier, C.,
737 Assefa, K., Tadele, Z., 2014. Genome and transcriptome sequencing identifies breeding targets in
738 the orphan crop tef (Eragrostis tef). BMC Genomics 15, 581. https://doi.org/10.1186/1471-2164-
739 15-581
740 Carballo, J., Santos, B. a. C.M., Zappacosta, D., Garbus, I., Selva, J.P., Gallo, C.A., Díaz, A., Albertini,
741 E., Caccamo, M., Echenique, V., 2019. A high-quality genome of Eragrostis curvula grass provides
742 insights into Poaceae evolution and supports new strategies to enhance forage quality. Sci. Rep.
743 9, 10250. https://doi.org/10.1038/s41598-019-46610-0
744 Chen, J., Huang, Q., Gao, D., Wang, Junyi, Lang, Y., Liu, T., Li, B., Bai, Z., Luis Goicoechea, J., Liang,
745 C., Chen, C., Zhang, W., Sun, S., Liao, Y., Zhang, X., Yang, L., Song, C., Wang, M., Shi, J., Liu,
746 G., Liu, J., Zhou, H., Zhou, W., Yu, Q., An, N., Chen, Y., Cai, Q., Wang, B., Liu, B., Min, J., Huang,
747 Y., Wu, H., Li, Z., Zhang, Y., Yin, Y., Song, W., Jiang, J., Jackson, S.A., Wing, R.A., Wang, Jun,
748 Chen, M., 2013. Whole-genome sequencing of Oryza brachyantha reveals mechanisms underlying
749 Oryza genome evolution. Nat. Commun. 4, 1595. https://doi.org/10.1038/ncomms2596
750 Chen, S., Zhou, Y., Chen, Y., Gu, J., 2018. fastp: an ultra-fast all-in-one FASTQ preprocessor.
751 Bioinformatics 34, i884–i890. https://doi.org/10.1093/bioinformatics/bty560
752 Cingolani, P., Platts, A., Wang, L.L., Coon, M., Nguyen, T., Wang, L., Land, S.J., Lu, X., Ruden, D.M.,
753 2012. A program for annotating and predicting the effects of single nucleotide polymorphisms,
754 SnpEff. Fly (Austin) 6, 80–92. https://doi.org/10.4161/fly.19695
755 Cock, P.J.A., Antao, T., Chang, J.T., Chapman, B.A., Cox, C.J., Dalke, A., Friedberg, I., Hamelryck, T.,
756 Kauff, F., Wilczynski, B., De Hoon, M.J.L., 2009. Biopython: freely available Python tools for
757 computational molecular biology and bioinformatics. Bioinformatics 25, 1422–1423.
758 https://doi.org/10.1093/bioinformatics/btp163
759 Danecek, P., Bonfield, J.K., Liddle, J., Marshall, J., Ohan, V., Pollard, M.O., Whitwham, A., Keane, T.,

McCarthy, S.A., Davies, R.M., Li, H., 2021. Twelve years of SAMtools and BCFtools. GigaScience 10, giab008. https://doi.org/10.1093/gigascience/giab008

De La Peña, R., Sattely, E.S., 2021. Rerouting plant terpene biosynthesis enables momilactone pathway elucidation. Nat. Chem. Biol. 17, 205–212. https://doi.org/10.1038/s41589-020-00669-3

Devos, K.M., Qi, P., Bahri, B.A., Gimode, D.M., Jenike, K., Manthi, S.J., Lule, D., Lux, T., Martinez-Bello, L., Pendergast, T.H., Plott, C., Saha, D., Sidhu, G.S., Sreedasyam, A., Wang, X., Wang, H., Wright, H., Zhao, J., Deshpande, S., de Villiers, S., Dida, M.M., Grimwood, J., Jenkins, J., Lovell, J., Mayer, K.F.X., Mneney, E.E., Ojulong, H.F., Schatz, M.C., Schmutz, J., Song, B., Tesfaye, K., Odeny, D.A., 2023. Genome analyses reveal population structure and a purple stigma color gene candidate in finger millet. Nat. Commun. 14, 3694. https://doi.org/10.1038/s41467-023-38915-6

Dobin, A., Davis, C.A., Schlesinger, F., Drenkow, J., Zaleski, C., Jha, S., Batut, P., Chaisson, M., Gingeras, T.R., 2013. STAR: ultrafast universal RNA-seq aligner. Bioinformatics 29, 15–21. https://doi.org/10.1093/bioinformatics/bts635

Dunning, L.T., Olofsson, J.K., Parisod, C., Choudhury, R.R., Moreno-Villena, J.J., Yang, Y., Dionora, J., Quick, W.P., Park, M., Bennetzen, J.L., Besnard, G., Nosil, P., Osborne, C.P., Christin, P.-A., 2019. Lateral transfers of large DNA fragments spread functional genes among grasses. Proc. Natl. Acad. Sci. 116, 4416–4425. https://doi.org/10.1073/pnas.1810031116

Emms, D.M., Kelly, S., 2019. OrthoFinder: phylogenetic orthology inference for comparative genomics. Genome Biol. 20, 238. https://doi.org/10.1186/s13059-019-1832-y

Emms, D.M., Kelly, S., 2018. STAG: Species Tree Inference from All Genes. https://doi.org/10.1101/267914

Emms, D.M., Kelly, S., 2015. OrthoFinder: solving fundamental biases in whole genome comparisons dramatically improves orthogroup inference accuracy. Genome Biol. 16, 157. https://doi.org/10.1186/s13059-015-0721-2

Ewels, P.A., Peltzer, A., Fillinger, S., Patel, H., Alneberg, J., Wilm, A., Garcia, M.U., Di Tommaso, P., Nahnsen, S., 2020. The nf-core framework for community-curated bioinformatics pipelines. Nat. Biotechnol. 38, 276–278. https://doi.org/10.1038/s41587-020-0439-x

Frerebeau, N., 2023. khroma: Colour Schemes for Scientific Data Visualization. Zenodo. https://doi.org/10.5281/zenodo.8269306

Garcia, M., Juhos, S., Larsson, M., Olason, P.I., Martin, M., Eisfeldt, J., DiLorenzo, S., Sandgren, J., Ståhl, T.D.D., Ewels, P., Wirta, V., Nistér, M., Käller, M., Nystedt, B., 2020. Sarek: A portable workflow for whole-genome sequencing analysis of germline and somatic variants. F1000Research. https://doi.org/10.12688/f1000research.16665.2

Ge, S., Sang, T., Lu, B.-R., Hong, D.-Y., 1999. Phylogeny of rice genomes with emphasis on origins of allotetraploid species. Proc. Natl. Acad. Sci. U. S. A. 96, 14400–14405.

Gordon, S.P., Contreras-Moreira, B., Levy, J.J., Djamei, A., Czedik-Eysenberg, A., Tartaglio, V.S., Session, A., Martin, J., Cartwright, A., Katz, A., Singan, V.R., Goltsman, E., Barry, K., Dinh-Thi, V.H., Chalhoub, B., Diaz-Perez, A., Sancho, R., Lusinska, J., Wolny, E., Nibau, C., Doonan, J.H., Mur, L.A.J., Plott, C., Jenkins, J., Hazen, S.P., Lee, S.J., Shu, S., Goodstein, D., Rokhsar, D., Schmutz, J., Hasterok, R., Catalan, P., Vogel, J.P., 2020. Gradual polyploid genome evolution revealed by pan-genomic analysis of Brachypodium hybridum and its diploid progenitors. Nat. Commun. 11, 3670. https://doi.org/10.1038/s41467-020-17302-5

Guo, L., Qiu, J., Ye, C., Jin, G., Mao, L., Zhang, H., Yang, X., Peng, Q., Wang, Yingying, Jia, L., Lin, Z., Li, G., Fu, F., Liu, C., Chen, L., Shen, E., Wang, W., Chu, Q., Wu, D., Wu, S., Xia, C., Zhang, Y., Zhou, X., Wang, L., Wu, L., Song, W., Wang, Yunfei, Shu, Q., Aoki, D., Yumoto, E., Yokota, T., Miyamoto, K., Okada, K., Kim, D.-S., Cai, D., Zhang, C., Lou, Y., Qian, Q., Yamaguchi, H., Yamane, H., Kong, C.-H., Timko, M.P., Bai, L., Fan, L., 2017. Echinochloa crus-galli genome analysis provides insight into its adaptation and invasiveness as a weed. Nat. Commun. 8, 1031. https://doi.org/10.1038/s41467-017-01067-5

Guo, Y.-L., Ge, S., 2005. Molecular phylogeny of Oryzeae (Poaceae) based on DNA sequences from chloroplast, mitochondrial, and nuclear genomes. Am. J. Bot. 92, 1548–1558. https://doi.org/10.3732/ajb.92.9.1548

Guo, Z.-H., Ma, P.-F., Yang, G.-Q., Hu, J.-Y., Liu, Y.-L., Xia, E.-H., Zhong, M.-C., Zhao, L., Sun, G.-L., Xu, Y.-X., Zhao, Y.-J., Zhang, Y.-C., Zhang, Y.-X., Zhang, X.-M., Zhou, M.-Y., Guo, Y., Guo, C., Liu, J.-X., Ye, X.-Y., Chen, Y.-M., Yang, Y., Han, B., Lin, C.-S., Lu, Y., Li, D.-Z., 2019. Genome Sequences Provide Insights into the Reticulate Origin and Unique Traits of Woody Bamboos. Mol.

Plant 12, 1353–1365. https://doi.org/10.1016/j.molp.2019.05.009
Haas, M., Kono, T., Macchietto, M., Millas, R., McGilp, L., Shao, M., Duquette, J., Qiu, Y., Hirsch, C.N., Kimball, J., 2021. Whole-genome assembly and annotation of northern wild rice, Zizania palustris L., supports a whole-genome duplication in the Zizania genus. Plant J. 107, 1802–1818. https://doi.org/10.1111/tpj.15419
Hibdige, S.G.S., Raimondeau, P., Christin, P.-A., Dunning, L.T., 2021. Widespread lateral gene transfer among grasses. New Phytol. 230, 2474–2486. https://doi.org/10.1111/nph.17328
Hoang, D.T., Chernomor, O., von Haeseler, A., Minh, B.Q., Vinh, L.S., 2018. UFBoot2: Improving the Ultrafast Bootstrap Approximation. Mol. Biol. Evol. 35, 518–522. https://doi.org/10.1093/molbev/msx281
Itoh, A., Nakazato, S., Wakabayashi, H., Hamano, A., Shenton, M.R., Miyamoto, K., Mitsuhashi, W., Okada, K., Toyomasu, T., 2021. Functional kaurene-synthase-like diterpene synthases lacking a gamma domain are widely present in Oryza and related species. Biosci. Biotechnol. Biochem. 85, 1945–1952. https://doi.org/10.1093/bbb/zbab127
Kajiya-Kanegae, H., Ohyanagi, H., Ebata, T., Tanizawa, Y., Onogi, A., Sawada, Y., Hirai, M.Y., Wang, Z.-X., Han, B., Toyoda, A., Fujiyama, A., Iwata, H., Tsuda, K., Suzuki, T., Nosaka-Takahashi, M., Nonomura, K., Nakamura, Y., Kawamoto, S., Kurata, N., Sato, Y., 2021. OryzaGenome2.1: Database of Diverse Genotypes in Wild Oryza Species. Rice 14, 24. https://doi.org/10.1186/s12284-021-00468-x
Kalyaanamoorthy, S., Minh, B.Q., Wong, T.K.F., von Haeseler, A., Jermiin, L.S., 2017. ModelFinder: fast model selection for accurate phylogenetic estimates. Nat. Methods 14, 587–589. https://doi.org/10.1038/nmeth.4285
Kato, T., Kabuto, C., Sasaki, N., Tsunagawa, M., Aizawa, H., Fujita, K., Kato, Y., Kitahara, Y., Takahashi, N., 1973. Momilactones, growth inhibitors from rice, oryza sativa L. Tetrahedron Lett. 14, 3861–3864. https://doi.org/10.1016/S0040-4039(01)87058-1
Katoh, K., Misawa, K., Kuma, K., Miyata, T., 2002. MAFFT: a novel method for rapid multiple sequence alignment based on fast Fourier transform. Nucleic Acids Res. 30, 3059–3066. https://doi.org/10.1093/nar/gkf436
Katoh, K., Standley, D.M., 2013. MAFFT Multiple Sequence Alignment Software Version 7: Improvements in Performance and Usability. Mol. Biol. Evol. 30, 772–780. https://doi.org/10.1093/molbev/mst010
Kato-Noguchi, H., Hasegawa, M., Ino, T., Ota, K., Kujime, H., 2010. Contribution of momilactone A and B to rice allelopathy. J. Plant Physiol. 167, 787–791. https://doi.org/10.1016/j.jplph.2010.01.014
Kato-Noguchi, H., Ino, T., 2003. Rice seedlings release momilactone B into the environment. Phytochemistry 63, 551–554. https://doi.org/10.1016/S0031-9422(03)00194-8
Kitaoka, N., Zhang, J., Oyagbenro, R.K., Brown, B., Wu, Y., Yang, B., Li, Z., Peters, R.J., 2021. Interdependent evolution of biosynthetic gene clusters for momilactone production in rice. Plant Cell 33, 290–305. https://doi.org/10.1093/plcell/koaa023
Kodama, O., Suzuki, T., Miyakawa, J., Akatsuka, T., 1988. Ultraviolet-Induced Accumulation of Phytoalexins in Rice Leaves. Agric. Biol. Chem. 52, 2469–2473. https://doi.org/10.1080/00021369.1988.10869067
Kraehmer, H., Jabran, K., Mennan, H., Chauhan, B.S., 2016. Global distribution of rice weeds – A review. Crop Prot. 80, 73–86. https://doi.org/10.1016/j.cropro.2015.10.027
Krueger, F., James, F., Ewels, P., Afyounian, E., Schuster-Boeckler, B., 2021. FelixKrueger/TrimGalore: v0.6.7 - DOI via Zenodo. https://doi.org/10.5281/zenodo.5127899
Liu, Y., Balcke, G.U., Porzel, A., Mahdi, L., Scherr-Henning, A., Bathe, U., Zuccaro, A., Tissier, A., 2021. A barley gene cluster for the biosynthesis of diterpenoid phytoalexins. bioRxiv. https://doi.org/10.1101/2021.05.21.445084
Liu, Z., Cheema, J., Vigouroux, M., Hill, L., Reed, J., Paajanen, P., Yant, L., Osbourn, A., 2020. Formation and diversification of a paradigm biosynthetic gene cluster in plants. Nat. Commun. 11, 5354. https://doi.org/10.1038/s41467-020-19153-6
Lovell, J.T., Jenkins, J., Lowry, D.B., Mamidi, S., Sreedasyam, A., Weng, X., Barry, K., Bonnette, J., Campitelli, B., Daum, C., Gordon, S.P., Gould, B.A., Khasanova, A., Lipzen, A., MacQueen, A., Palacio-Mejía, J.D., Plott, C., Shakirov, E.V., Shu, S., Yoshinaga, Y., Zane, M., Kudrna, D., Talag, J.D., Rokhsar, D., Grimwood, J., Schmutz, J., Juenger, T.E., 2018. The genomic landscape of molecular responses to natural drought stress in Panicum hallii. Nat. Commun. 9, 5213.

https://doi.org/10.1038/s41467-018-07669-x
Lovell, J.T., MacQueen, A.H., Mamidi, S., Bonnette, J., Jenkins, J., Napier, J.D., Sreedasyam, A., Healey, A., Session, A., Shu, S., Barry, K., Bonos, S., Boston, L., Daum, C., Deshpande, S., Ewing, A., Grabowski, P.P., Haque, T., Harrison, M., Jiang, J., Kudrna, D., Lipzen, A., Pendergast, T.H., Plott, C., Qi, P., Saski, C.A., Shakirov, E.V., Sims, D., Sharma, M., Sharma, R., Stewart, A., Singan, V.R., Tang, Y., Thibivillier, S., Webber, J., Weng, X., Williams, M., Wu, G.A., Yoshinaga, Y., Zane, M., Zhang, L., Zhang, J., Behrman, K.D., Boe, A.R., Fay, P.A., Fritschi, F.B., Jastrow, J.D., Lloyd-Reilley, J., Martínez-Reyna, J.M., Matamala, R., Mitchell, R.B., Rouquette, F.M., Ronald, P., Saha, M., Tobias, C.M., Udvardi, M., Wing, R.A., Wu, Y., Bartley, L.E., Casler, M., Devos, K.M., Lowry, D.B., Rokhsar, D.S., Grimwood, J., Juenger, T.E., Schmutz, J., 2021. Genomic mechanisms of climate adaptation in polyploid bioenergy switchgrass. Nature 590, 438–444. https://doi.org/10.1038/s41586-020-03127-1
Lu, F., Ammiraju, J.S.S., Sanyal, A., Zhang, S., Song, R., Chen, J., Li, G., Sui, Y., Song, X., Cheng, Z., Oliveira, A.C. de, Bennetzen, J.L., Jackson, S.A., Wing, R.A., Chen, M., 2009. Comparative sequence analysis of MONOCULM1-orthologous regions in 14 Oryza genomes. Proc. Natl. Acad. Sci. 106, 2071–2076. https://doi.org/10.1073/pnas.0812798106
Ma, P.-F., Liu, Y.-L., Jin, G.-H., Liu, J.-X., Wu, H., He, J., Guo, Z.-H., Li, D.-Z., 2021. The Pharus latifolius genome bridges the gap of early grass evolution. Plant Cell 33, 846–864. https://doi.org/10.1093/plcell/koab015
Mascher, M., Wicker, T., Jenkins, J., Plott, C., Lux, T., Koh, C.S., Ens, J., Gundlach, H., Boston, L.B., Tulpová, Z., Holden, S., Hernández-Pinzón, I., Scholz, U., Mayer, K.F.X., Spannagl, M., Pozniak, C.J., Sharpe, A.G., Šimková, H., Moscou, M.J., Grimwood, J., Schmutz, J., Stein, N., 2021. Long-read sequence assembly: a technical evaluation in barley. Plant Cell 33, 1888–1906. https://doi.org/10.1093/plcell/koab077
McCormick, R.F., Truong, S.K., Sreedasyam, A., Jenkins, J., Shu, S., Sims, D., Kennedy, M., Amirebrahimi, M., Weers, B.D., McKinley, B., Mattison, A., Morishige, D.T., Grimwood, J., Schmutz, J., Mullet, J.E., 2018. The Sorghum bicolor reference genome: improved assembly, gene annotations, a transcriptome atlas, and signatures of genome organization. Plant J. 93, 338–354. https://doi.org/10.1111/tpj.13781
McKenna, A., Hanna, M., Banks, E., Sivachenko, A., Cibulskis, K., Kernytsky, A., Garimella, K., Altshuler, D., Gabriel, S., Daly, M., DePristo, M.A., 2010. The Genome Analysis Toolkit: A MapReduce framework for analyzing next-generation DNA sequencing data. Genome Res. 20, 1297–1303. https://doi.org/10.1101/gr.107524.110
Ming, R., VanBuren, R., Wai, C.M., Tang, H., Schatz, M.C., Bowers, J.E., Lyons, E., Wang, M.-L., Chen, J., Biggers, E., Zhang, Jisen, Huang, L., Zhang, L., Miao, W., Zhang, Jian, Ye, Z., Miao, C., Lin, Z., Wang, H., Zhou, H., Yim, W.C., Priest, H.D., Zheng, C., Woodhouse, M., Edger, P.P., Guyot, R., Guo, H.-B., Guo, H., Zheng, G., Singh, R., Sharma, A., Min, X., Zheng, Y., Lee, H., Gurtowski, J., Sedlazeck, F.J., Harkess, A., McKain, M.R., Liao, Z., Fang, J., Liu, J., Zhang, X., Zhang, Q., Hu, W., Qin, Y., Wang, K., Chen, L.-Y., Shirley, N., Lin, Y.-R., Liu, L.-Y., Hernandez, A.G., Wright, C.L., Bulone, V., Tuskan, G.A., Heath, K., Zee, F., Moore, P.H., Sunkar, R., Leebens-Mack, J.H., Mockler, T., Bennetzen, J.L., Freeling, M., Sankoff, D., Paterson, A.H., Zhu, X., Yang, X., Smith, J.A.C., Cushman, J.C., Paull, R.E., Yu, Q., 2015. The pineapple genome and the evolution of CAM photosynthesis. Nat. Genet. 47, 1435–1442. https://doi.org/10.1038/ng.3435
Minh, B.Q., Schmidt, H.A., Chernomor, O., Schrempf, D., Woodhams, M.D., von Haeseler, A., Lanfear, R., 2020. IQ-TREE 2: New Models and Efficient Methods for Phylogenetic Inference in the Genomic Era. Mol. Biol. Evol. 37, 1530–1534. https://doi.org/10.1093/molbev/msaa015
Miyamoto, K., Fujita, M., Shenton, M.R., Akashi, S., Sugawara, C., Sakai, A., Horie, K., Hasegawa, M., Kawaide, H., Mitsuhashi, W., Nojiri, H., Yamane, H., Kurata, N., Okada, K., Toyomasu, T., 2016. Evolutionary trajectory of phytoalexin biosynthetic gene clusters in rice. Plant J. 87, 293–304. https://doi.org/10.1111/tpj.13200
Nützmann, H.-W., Huang, A., Osbourn, A., 2016. Plant metabolic clusters – from genetics to genomics. New Phytol. 211, 771–789. https://doi.org/10.1111/nph.13981
Okada, K., 2011. The Biosynthesis of Isoprenoids and the Mechanisms Regulating It in Plants. Biosci. Biotechnol. Biochem. 75, 1219–1225. https://doi.org/10.1271/bbb.110228
Otomo, K., Kanno, Y., Motegi, A., Kenmoku, H., Yamane, H., Mitsuhashi, W., Oikawa, H., Toshima, H., Itoh, H., Matsuoka, M., Sassa, T., Toyomasu, T., 2004a. Diterpene Cyclases Responsible for the

Biosynthesis of Phytoalexins, Momilactones A, B, and Oryzalexins A–F in Rice. Biosci. Biotechnol. Biochem. 68, 2001–2006. https://doi.org/10.1271/bbb.68.2001

Otomo, K., Kenmoku, H., Oikawa, H., König, W.A., Toshima, H., Mitsuhashi, W., Yamane, H., Sassa, T., Toyomasu, T., 2004b. Biological functions of ent- and syn-copalyl diphosphate synthases in rice: key enzymes for the branch point of gibberellin and phytoalexin biosynthesis. Plant J. 39, 886–893. https://doi.org/10.1111/j.1365-313X.2004.02175.x

Ouyang, S., Zhu, W., Hamilton, J., Lin, H., Campbell, M., Childs, K., Thibaud-Nissen, F., Malek, R.L., Lee, Y., Zheng, L., Orvis, J., Haas, B., Wortman, J., Buell, C.R., 2007. The TIGR Rice Genome Annotation Resource: improvements and new features. Nucleic Acids Res. 35, D883–D887. https://doi.org/10.1093/nar/gkl976

Patel, H., Ewels, P., Peltzer, A., Manning, J., Botvinnik, O., Sturm, G., Garcia, M.U., Moreno, D., Vemuri, P., bot, nf-core, Binzer-Panchal, M., silviamorins, Pantano, L., Zepper, M., Syme, R., Talbot, A., Kelly, G., Hanssen, F., Yates, J.A.F., Espinosa-Carrasco, J., rfenouil, Cheshire, C., marchoeppner, Miller, E., Zhou, P., Guinchard, S., Gabernet, G., Mertes, C., Straub, D., Tommaso, P.D., 2024. nf-core/rnaseq: nf-core/rnaseq v3.14.0 - Hassium Honey Badger. https://doi.org/10.5281/zenodo.10471647

Patro, R., Duggal, G., Love, M.I., Irizarry, R.A., Kingsford, C., 2017. Salmon provides fast and bias-aware quantification of transcript expression. Nat. Methods 14, 417–419. https://doi.org/10.1038/nmeth.4197

Pertea, G., Pertea, M., 2020. GFF Utilities: GffRead and GffCompare. F1000Research. https://doi.org/10.12688/f1000research.23297.1

Phillips, A.L., Ferguson, S., Watson-Haigh, N.S., Jones, A.W., Borevitz, J.O., Burton, R.A., Atwell, B.J., 2022. The first long-read nuclear genome assembly of Oryza australiensis, a wild rice from northern Australia. Sci. Rep. 12, 10823. https://doi.org/10.1038/s41598-022-14893-5

Polturak, G., Dippe, M., Stephenson, M.J., Chandra Misra, R., Owen, C., Ramirez-Gonzalez, R.H., Haidoulis, J.F., Schoonbeek, H.-J., Chartrain, L., Borrill, P., Nelson, D.R., Brown, J.K.M., Nicholson, P., Uauy, C., Osbourn, A., 2022a. Pathogen-induced biosynthetic pathways encode defense-related molecules in bread wheat. Proc. Natl. Acad. Sci. 119, e2123299119. https://doi.org/10.1073/pnas.2123299119

Polturak, G., Liu, Z., Osbourn, A., 2022b. New and emerging concepts in the evolution and function of plant biosynthetic gene clusters. Curr. Opin. Green Sustain. Chem. 33, 100568. https://doi.org/10.1016/j.cogsc.2021.100568

Poplin, R., Ruano-Rubio, V., DePristo, M.A., Fennell, T.J., Carneiro, M.O., Auwera, G.A.V. der, Kling, D.E., Gauthier, L.D., Levy-Moonshine, A., Roazen, D., Shakir, K., Thibault, J., Chandran, S., Whelan, C., Lek, M., Gabriel, S., Daly, M.J., Neale, B., MacArthur, D.G., Banks, E., 2018. Scaling accurate genetic variant discovery to tens of thousands of samples. bioRxiv 201178. https://doi.org/10.1101/201178

Rabanus-Wallace, M.T., Hackauf, B., Mascher, M., Lux, T., Wicker, T., Gundlach, H., Baez, M., Houben, A., Mayer, K.F.X., Guo, L., Poland, J., Pozniak, C.J., Walkowiak, S., Melonek, J., Praz, C.R., Schreiber, M., Budak, H., Heuberger, M., Steuernagel, B., Wulff, B., Börner, A., Byrns, B., Čížková, J., Fowler, D.B., Fritz, A., Himmelbach, A., Kaithakottil, G., Keilwagen, J., Keller, B., Konkin, D., Larsen, J., Li, Q., Myśków, B., Padmarasu, S., Rawat, N., Sesiz, U., Biyiklioglu-Kaya, S., Sharpe, A., Šimková, H., Small, I., Swarbreck, D., Toegelová, H., Tsvetkova, N., Voylokov, A.V., Vrána, J., Bauer, E., Bolibok-Bragoszewska, H., Doležel, J., Hall, A., Jia, J., Korzun, V., Laroche, A., Ma, X.-F., Ordon, F., Özkan, H., Rakoczy-Trojanowska, M., Scholz, U., Schulman, A.H., Siekmann, D., Stojałowski, S., Tiwari, V.K., Spannagl, M., Stein, N., 2021. Chromosome-scale genome assembly provides insights into rye biology, evolution and agronomic potential. Nat. Genet. 53, 564–573. https://doi.org/10.1038/s41588-021-00807-0

Schnable, P.S., Ware, D., Fulton, R.S., Stein, J.C., Wei, F., Pasternak, S., Liang, C., Zhang, J., Fulton, L., Graves, T.A., Minx, P., Reily, A.D., Courtney, L., Kruchowski, S.S., Tomlinson, C., Strong, C., Delehaunty, K., Fronick, C., Courtney, B., Rock, S.M., Belter, E., Du, F., Kim, K., Abbott, R.M., Cotton, M., Levy, A., Marchetto, P., Ochoa, K., Jackson, S.M., Gillam, B., Chen, W., Yan, L., Higginbotham, J., Cardenas, M., Waligorski, J., Applebaum, E., Phelps, L., Falcone, J., Kanchi, K., Thane, T., Scimone, A., Thane, N., Henke, J., Wang, T., Ruppert, J., Shah, N., Rotter, K., Hodges, J., Ingenthron, E., Cordes, M., Kohlberg, S., Sgro, J., Delgado, B., Mead, K., Chinwalla, A., Leonard, S., Crouse, K., Collura, K., Kudrna, D., Currie, J., He, R., Angelova, A., Rajasekar, S.,

Mueller, T., Lomeli, R., Scara, G., Ko, A., Delaney, K., Wissotski, M., Lopez, G., Campos, D., Braidotti, M., Ashley, E., Golser, W., Kim, H., Lee, S., Lin, J., Dujmic, Z., Kim, W., Talag, J., Zuccolo, A., Fan, C., Sebastian, A., Kramer, M., Spiegel, L., Nascimento, L., Zutavern, T., Miller, B., Ambroise, C., Muller, S., Spooner, W., Narechania, A., Ren, L., Wei, S., Kumari, S., Faga, B., Levy, M.J., McMahan, L., Van Buren, P., Vaughn, M.W., Ying, K., Yeh, C.-T., Emrich, S.J., Jia, Y., Kalyanaraman, A., Hsia, A.-P., Barbazuk, W.B., Baucom, R.S., Brutnell, T.P., Carpita, N.C., Chaparro, C., Chia, J.-M., Deragon, J.-M., Estill, J.C., Fu, Y., Jeddeloh, J.A., Han, Y., Lee, H., Li, P., Lisch, D.R., Liu, S., Liu, Z., Nagel, D.H., McCann, M.C., SanMiguel, P., Myers, A.M., Nettleton, D., Nguyen, J., Penning, B.W., Ponnala, L., Schneider, K.L., Schwartz, D.C., Sharma, A., Soderlund, C., Springer, N.M., Sun, Q., Wang, H., Waterman, M., Westerman, R., Wolfgruber, T.K., Yang, L., Yu, Y., Zhang, L., Zhou, S., Zhu, Q., Bennetzen, J.L., Dawe, R.K., Jiang, J., Jiang, N., Presting, G.G., Wessler, S.R., Aluru, S., Martienssen, R.A., Clifton, S.W., McCombie, W.R., Wing, R.A., Wilson, R.K., 2009. The B73 Maize Genome: Complexity, Diversity, and Dynamics. Science 326, 1112–1115. https://doi.org/10.1126/science.1178534

Serra Serra, N., Schanmuganathan, R., Becker, C. 2021. Allelopathy in rice: a story on momilactones, kin recognition, and weed management. J. Exp. Bot. erab084. https://doi.org/10.1093/jxb/erab084.

Shenton, M., Kobayashi, M., Terashima, S., Ohyanagi, H., Copetti, D., Hernández-Hernández, T., Zhang, J., Ohmido, N., Fujita, M., Toyoda, A., Ikawa, H., Fujiyama, A., Furuumi, H., Miyabayashi, T., Kubo, T., Kudrna, D., Wing, R., Yano, K., Nonomura, K.-I., Sato, Y., Kurata, N., 2020. Evolution and Diversity of the Wild Rice Oryza officinalis Complex, across Continents, Genome Types, and Ploidy Levels. Genome Biol. Evol. 12, 413–428. https://doi.org/10.1093/gbe/evaa037

Shi, C., Li, W., Zhang, Q.-J., Zhang, Y., Tong, Y., Li, K., Liu, Y.-L., Gao, L.-Z., 2020. The draft genome sequence of an upland wild rice species, Oryza granulata. Sci. Data 7, 131. https://doi.org/10.1038/s41597-020-0470-2

Shimura, K., Okada, A., Okada, K., Jikumaru, Y., Ko, K.-W., Toyomasu, T., Sassa, T., Hasegawa, M., Kodama, O., Shibuya, N., Koga, J., Nojiri, H., Yamane, H., 2007. Identification of a Biosynthetic Gene Cluster in Rice for Momilactones. J. Biol. Chem. 282, 34013–34018. https://doi.org/10.1074/jbc.M703344200

Smit, S.J., Lichman, B.R., 2022. Plant biosynthetic gene clusters in the context of metabolic evolution. Nat. Prod. Rep. https://doi.org/10.1039/D2NP00005A

Soreng, R.J., Peterson, P.M., Romaschenko, K., Davidse, G., Teisher, J.K., Clark, L.G., Barberá, P., Gillespie, L.J., Zuloaga, F.O., 2017. A worldwide phylogenetic classification of the Poaceae (Gramineae) II: An update and a comparison of two 2015 classifications. J. Syst. Evol. 55, 259–290. https://doi.org/10.1111/jse.12262

Sreedasyam, A., Plott, C., Hossain, M.S., Lovell, J.T., Grimwood, J., Jenkins, J.W., Daum, C., Barry, K., Carlson, J., Shu, S., Phillips, J., Amirebrahimi, M., Zane, M., Wang, M., Goodstein, D., Haas, F.B., Hiss, M., Perroud, P.-F., Jawdy, S.S., Yang, Y., Hu, R., Johnson, J., Kropat, J., Gallaher, S.D., Lipzen, A., Shakirov, E.V., Weng, X., Torres-Jerez, I., Weers, B., Conde, D., Pappas, M.R., Liu, L., Muchlinski, A., Jiang, H., Shyu, C., Huang, P., Sebastian, J., Laiben, C., Medlin, A., Carey, S., Carrell, A.A., Chen, J.-G., Perales, M., Swaminathan, K., Allona, I., Grattapaglia, D., Cooper, E.A., Tholl, D., Vogel, J.P., Weston, D.J., Yang, X., Brutnell, T.P., Kellogg, E.A., Baxter, I., Udvardi, M., Tang, Y., Mockler, T.C., Juenger, T.E., Mullet, J., Rensing, S.A., Tuskan, G.A., Merchant, S.S., Stacey, G., Schmutz, J., 2023. JGI Plant Gene Atlas: an updateable transcriptome resource to improve functional gene descriptions across the plant kingdom. Nucleic Acids Res. 51, 8383–8401. https://doi.org/10.1093/nar/gkad616

Stein, J.C., Yu, Y., Copetti, D., Zwickl, D.J., Zhang, L., Zhang, C., Chougule, K., Gao, D., Iwata, A., Goicoechea, J.L., Wei, S., Wang, J., Liao, Y., Wang, M., Jacquemin, J., Becker, C., Kudrna, D., Zhang, J., Londono, C.E.M., Song, X., Lee, S., Sanchez, P., Zuccolo, A., Ammiraju, J.S.S., Talag, J., Danowitz, A., Rivera, L.F., Gschwend, A.R., Noutsos, C., Wu, C., Kao, S., Zeng, J., Wei, F., Zhao, Q., Feng, Q., El Baidouri, M., Carpentier, M.-C., Lasserre, E., Cooke, R., Rosa Farias, D. da, da Maia, L.C., dos Santos, R.S., Nyberg, K.G., McNally, K.L., Mauleon, R., Alexandrov, N., Schmutz, J., Flowers, D., Fan, C., Weigel, D., Jena, K.K., Wicker, T., Chen, M., Han, B., Henry, R., Hsing, Y.C., Kurata, N., de Oliveira, A.C., Panaud, O., Jackson, S.A., Machado, C.A., Sanderson, M.J., Long, M., Ware, D., Wing, R.A., 2018. Genomes of 13 domesticated and wild rice relatives highlight genetic conservation, turnover and innovation across the genus Oryza. Nat. Genet. 50, 285–296. https://doi.org/10.1038/s41588-018-0040-0

Sun, G., Wase, N., Shu, S., Jenkins, J., Zhou, B., Torres-Rodríguez, J.V., Chen, C., Sandor, L., Plott, C., Yoshinga, Y., Daum, C., Qi, P., Barry, K., Lipzen, A., Berry, L., Pedersen, C., Gottilla, T., Foltz, A., Yu, H., O'Malley, R., Zhang, C., Devos, K.M., Sigmon, B., Yu, B., Obata, T., Schmutz, J., Schnable, J.C., 2022. Genome of Paspalum vaginatum and the role of trehalose mediated autophagy in increasing maize biomass. Nat. Commun. 13, 7731. https://doi.org/10.1038/s41467-022-35507-8

Tamogani, S., Mitani, M., Kodama, O., Akatsuka, T., 1993. Oryzalexin S structure: a new stemarane-type rice plant phytoalexin and its biogenesis. Tetrahedron 49, 2025–2032. https://doi.org/10.1016/S0040-4020(01)86302-X

Toyomasu, T., Goda, C., Sakai, A., Miyamoto, K., Shenton, M.R., Tomiyama, S., Mitsuhashi, W., Yamane, H., Kurata, N., Okada, K., 2018. Characterization of diterpene synthase genes in the wild rice species *Oryza brachyatha* provides evolutionary insight into rice phytoalexin biosynthesis. Biochem. Biophys. Res. Commun. 503, 1221–1227. https://doi.org/10.1016/j.bbrc.2018.07.028

Toyomasu, T., Miyamoto, K., Shenton, M.R., Sakai, A., Sugawara, C., Horie, K., Kawaide, H., Hasegawa, M., Chuba, M., Mitsuhashi, W., Yamane, H., Kurata, N., Okada, K., 2016. Characterization and evolutionary analysis of ent-kaurene synthase like genes from the wild rice species Oryza rufipogon. Biochem. Biophys. Res. Commun. 480, 402–408. https://doi.org/10.1016/j.bbrc.2016.10.062

Toyomasu, T., Shenton, M.R., Okada, K., 2020. Evolution of Labdane-Related Diterpene Synthases in Cereals. Plant Cell Physiol. 61, 1850–1859. https://doi.org/10.1093/pcp/pcaa106

Toyomasu, T., Tsukahara, M., Kaneko, A., Niida, R., Mitsuhashi, W., Dairi, T., Kato, N., Sassa, T., 2007. Fusicoccins are biosynthesized by an unusual chimera diterpene synthase in fungi. Proc. Natl. Acad. Sci. 104, 3084–3088. https://doi.org/10.1073/pnas.0608426104

VanBuren, R., Bryant, D., Edger, P.P., Tang, H., Burgess, D., Challabathula, D., Spittle, K., Hall, R., Gu, J., Lyons, E., Freeling, M., Bartels, D., Ten Hallers, B., Hastie, A., Michael, T.P., Mockler, T.C., 2015. Single-molecule sequencing of the desiccation-tolerant grass Oropetium thomaeum. Nature 527, 508–511. https://doi.org/10.1038/nature15714

Vogel, J.P., Garvin, D.F., Mockler, T.C., Schmutz, J., Rokhsar, D., Bevan, M.W., Barry, K., Lucas, S., Harmon-Smith, M., Lail, K., Tice, H., Schmutz (Leader), J., Grimwood, J., McKenzie, N., Bevan, M.W., Huo, N., Gu, Y.Q., Lazo, G.R., Anderson, O.D., Vogel (Leader), J.P., You, F.M., Luo, M.-C., Dvorak, J., Wright, J., Febrer, M., Bevan, M.W., Idziak, D., Hasterok, R., Garvin, D.F., Lindquist, E., Wang, M., Fox, S.E., Priest, H.D., Filichkin, S.A., Givan, S.A., Bryant, D.W., Chang, J.H., Mockler (Leader), T.C., Wu, H., Wu, W., Hsia, A.-P., Schnable, P.S., Kalyanaraman, A., Barbazuk, B., Michael, T.P., Hazen, S.P., Bragg, J.N., Laudencia-Chingcuanco, D., Vogel, J.P., Garvin, D.F., Weng, Y., McKenzie, N., Bevan, M.W., Haberer, G., Spannagl, M., Mayer (Leader), K., Rattei, T., Mitros, T., Rokhsar, D., Lee, S.-J., Rose, J.K.C., Mueller, L.A., York, T.L., Wicker (Leader), T., Buchmann, J.P., Tanskanen, J., Schulman (Leader), A.H., Gundlach, H., Wright, J., Bevan, M., Costa de Oliveira, A., da C. Maia, L., Belknap, W., Gu, Y.Q., Jiang, N., Lai, J., Zhu, L., Ma, J., Sun, C., Pritham, E., Salse (Leader), J., Murat, F., Abrouk, M., Haberer, G., Spannagl, M., Mayer, K., Bruggmann, R., Messing, J., You, F.M., Luo, M.-C., Dvorak, J., Fahlgren, N., Fox, S.E., Sullivan, C.M., Mockler, T.C., Carrington, J.C., Chapman, E.J., May, G.D., Zhai, J., Ganssmann, M., Guna Ranjan Gurazada, S., German, M., Meyers, B.C., Green (Leader), P.J., Bragg, J.N., Tyler, L., Wu, J., Gu, Y.Q., Lazo, G.R., Laudencia-Chingcuanco, D., Thomson, J., Vogel (Leader), J.P., Hazen, S.P., Chen, S., Scheller, H.V., Harholt, J., Ulvskov, P., Fox, S.E., Filichkin, S.A., Fahlgren, N., Kimbrel, J.A., Chang, J.H., Sullivan, C.M., Chapman, E.J., Carrington, J.C., Mockler, T.C., Bartley, L.E., Cao, P., Jung, K.-H., Sharma, M.K., Vega-Sanchez, M., Ronald, P., Dardick, C.D., De Bodt, S., Verelst, W., Inzé, D., Heese, M., Schnittger, A., Yang, X., Kalluri, U.C., Tuskan, G.A., Hua, Z., Vierstra, R.D., Garvin, D.F., Cui, Y., Ouyang, S., Sun, Q., Liu, Z., Yilmaz, A., Grotewold, E., Sibout, R., Hematy, K., Mouille, G., Höfte, H., Michael, T., Pelloux, J., O'Connor, D., Schnable, J., Rowe, S., Harmon, F., Cass, C.L., Sedbrook, J.C., Byrne, M.E., Walsh, S., Higgins, J., Bevan, M., Li, P., Brutnell, T., Unver, T., Budak, H., Belcram, H., Charles, M., Chalhoub, B., Baxter, I., The International Brachypodium Initiative, Principal investigators, DNA sequencing and assembly, Pseudomolecule assembly and BAC end sequencing, Transcriptome sequencing and analysis, Gene analysis and annotation, Repeats analysis, Comparative genomics, Small RNA analysis, Manual annotation and gene family analysis, 2010. Genome sequencing and analysis of the model grass Brachypodium distachyon. Nature 463, 763–768. https://doi.org/10.1038/nature08747

Wang, L., Zhu, T., Rodriguez, J.C., Deal, K.R., Dubcovsky, J., McGuire, P.E., Lux, T., Spannagl, M., Mayer, K.F.X., Baldrich, P., Meyers, B.C., Huo, N., Gu, Y.Q., Zhou, H., Devos, K.M., Bennetzen, J.L., Unver, T., Budak, H., Gulick, P.J., Galiba, G., Kalapos, B., Nelson, D.R., Li, P., You, F.M., Luo, M.-C., Dvorak, J., 2021. Aegilops tauschii genome assembly Aet v5.0 features greater sequence contiguity and improved annotation. G3 GenesGenomesGenetics 11, jkab325. https://doi.org/10.1093/g3journal/jkab325

Wickham, H., Averick, M., Bryan, J., Chang, W., McGowan, L.D., François, R., Grolemund, G., Hayes, A., Henry, L., Hester, J., Kuhn, M., Pedersen, T.L., Miller, E., Bache, S.M., Müller, K., Ooms, J., Robinson, D., Seidel, D.P., Spinu, V., Takahashi, K., Vaughan, D., Wilke, C., Woo, K., Yutani, H., 2019. Welcome to the Tidyverse. J. Open Source Softw. 4, 1686. https://doi.org/10.21105/joss.01686

Wilderman, P.R., Xu, M., Jin, Y., Coates, R.M., Peters, R.J., 2004. Identification of Syn-Pimara-7,15-Diene Synthase Reveals Functional Clustering of Terpene Synthases Involved in Rice Phytoalexin/Allelochemical Biosynthesis. Plant Physiol. 135, 2098–2105. https://doi.org/10.1104/pp.104.045971

Wu, D., Hu, Y., Akashi, S., Nojiri, H., Guo, L., Ye, C.-Y., Zhu, Q.-H., Okada, K., Fan, L., 2022a. Lateral transfers lead to the birth of momilactone biosynthetic gene clusters in grass. Plant J. 111, 1354–1367. https://doi.org/10.1111/tpj.15893

Wu, D., Shen, E., Jiang, B., Feng, Y., Tang, W., Lao, S., Jia, L., Lin, H.-Y., Xie, L., Weng, X., Dong, C., Qian, Q., Lin, F., Xu, H., Lu, H., Cutti, L., Chen, H., Deng, S., Guo, L., Chuah, T.-S., Song, B.-K., Scarabel, L., Qiu, J., Zhu, Q.-H., Yu, Q., Timko, M.P., Yamaguchi, H., Merotto, A., Qiu, Y., Olsen, K.M., Fan, L., Ye, C.-Y., 2022b. Genomic insights into the evolution of Echinochloa species as weed and orphan crop. Nat. Commun. 13, 689. https://doi.org/10.1038/s41467-022-28359-9

Xu, M., Hillwig, M.L., Prisic, S., Coates, R.M., Peters, R.J., 2004. Functional identification of rice syn-copalyl diphosphate synthase and its role in initiating biosynthesis of diterpenoid phytoalexin/allelopathic natural products. Plant J. 39, 309–318. https://doi.org/10.1111/j.1365-313X.2004.02137.x

Yan, N., Yang, T., Yu, X.-T., Shang, L.-G., Guo, D.-P., Zhang, Y., Meng, L., Qi, Q.-Q., Li, Y.-L., Du, Y.-M., Liu, X.-M., Yuan, X.-L., Qin, P., Qiu, J., Qian, Q., Zhang, Z.-F., 2022. Chromosome-level genome assembly of Zizania latifolia provides insights into its seed shattering and phytocassane biosynthesis. Commun. Biol. 5, 1–11. https://doi.org/10.1038/s42003-021-02993-3

Yang, X., Gao, S., Guo, L., Wang, B., Jia, Y., Zhou, J., Che, Y., Jia, P., Lin, J., Xu, T., Sun, J., Ye, K., 2021. Three chromosome-scale Papaver genomes reveal punctuated patchwork evolution of the morphinan and noscapine biosynthesis pathway. Nat. Commun. 12, 6030. https://doi.org/10.1038/s41467-021-26330-8

Ye, Z., Nakagawa, K., Natsume, M., Nojiri, H., Kawaide, H., Okada, K. 2017. Biochemical synthesis of uniformly ^{13}C-labeled diterpene hydrocarbons and their bioconversion to diterpenoid phytoalexins in planta. Biosci. Biotechnol. Biochem. 81, 1176-1184. https://doi.org/10.1080/09168451.2017.1285689

Ye, C.-Y., Wu, D., Mao, L., Jia, L., Qiu, J., Lao, S., Chen, M., Jiang, B., Tang, W., Peng, Q., Pan, L., Wang, L., Feng, X., Guo, L., Zhang, C., Kellogg, E.A., Olsen, K.M., Bai, L., Fan, L., 2020. The Genomes of the Allohexaploid Echinochloa crus-galli and Its Progenitors Provide Insights into Polyploidization-Driven Adaptation. Mol. Plant 13, 1298–1310. https://doi.org/10.1016/j.molp.2020.07.001

Yu, H., Lin, T., Meng, X., Du, H., Zhang, J., Liu, G., Chen, Mingjiang, Jing, Y., Kou, L., Li, X., Gao, Q., Liang, Yan, Liu, X., Fan, Z., Liang, Yuntao, Cheng, Z., Chen, Mingsheng, Tian, Z., Wang, Y., Chu, C., Zuo, J., Wan, J., Qian, Q., Han, B., Zuccolo, A., Wing, R.A., Gao, C., Liang, C., Li, J., 2021. A route to de novo domestication of wild allotetraploid rice. Cell 184, 1156-1170.e14. https://doi.org/10.1016/j.cell.2021.01.013

Zhang, J., Wu, F., Yan, Q., John, U.P., Cao, M., Xu, P., Zhang, Z., Ma, T., Zong, X., Li, J., Liu, R., Zhang, Y., Zhao, Y., Kanzana, G., Lv, Y., Nan, Z., Spangenberg, G., Wang, Y., 2021. The genome of Cleistogenes songorica provides a blueprint for functional dissection of dimorphic flower differentiation and drought adaptability. Plant Biotechnol. J. 19, 532–547. https://doi.org/10.1111/pbi.13483

Zhao, H., Gao, Z., Wang, L., Wang, J., Wang, Songbo, Fei, B., Chen, C., Shi, C., Liu, X., Zhang, H., Lou, Y., Chen, L., Sun, H., Zhou, X., Wang, Sining, Zhang, C., Xu, H., Li, L., Yang, Y., Wei, Y.,

Yang, W., Gao, Q., Yang, H., Zhao, S., Jiang, Z., 2018. Chromosome-level reference genome and alternative splicing atlas of moso bamboo (Phyllostachys edulis). GigaScience 7, giy115. https://doi.org/10.1093/gigascience/giy115

Zhao, H., Wang, W., Yang, Y., Wang, Z., Sun, J., Yuan, K., Rabbi, S.M.H.A., Khanam, M., Kabir, M.S., Seraj, Z.I., Rahman, M.S., Zhang, Z., 2023. A high-quality chromosome-level wild rice genome of Oryza coarctata. Sci. Data 10, 701. https://doi.org/10.1038/s41597-023-02594-1

Zhou, Y., Ma, Y., Zeng, J., Duan, L., Xue, X., Wang, H., Lin, T., Liu, Z., Zeng, K., Zhong, Y., Zhang, S., Hu, Q., Liu, M., Zhang, H., Reed, J., Moses, T., Liu, Xinyan, Huang, P., Qing, Z., Liu, Xiubin, Tu, P., Kuang, H., Zhang, Z., Osbourn, A., Ro, D.-K., Shang, Y., Huang, S., 2016. Convergence and divergence of bitterness biosynthesis and regulation in Cucurbitaceae. Nat. Plants 2, 1–8. https://doi.org/10.1038/nplants.2016.183

Zi, J., Mafu, S., Peters, R.J., 2014. To Gibberellins and Beyond! Surveying the Evolution of (Di)Terpenoid Metabolism. Annu. Rev. Plant Biol. 65, 259–286. https://doi.org/10.1146/annurev-arplant-050213-035705

AUTHOR CONTRIBUTIONS

S.P.C. and C.B. conceived the study. S.P.C. carried out the genomic and phylogenetic analyses. T.T. and Y.H. carried out in vitro enzymatic assays. the functional analysis of KSL4. Y.L. and K.O. carried out momilactone measurements. H.N., K.O., and C.B. supervised the work. S.P.C. and C.B. wrote the manuscript with contributions from all authors.

ACKNOWLEDGEMENTS

We are grateful to José Villaécija Aguilar and Niklas Schandry for critical reading of the manuscript and to Niklas Schandry for setting up and maintaining environments for computational analyses. We would like to thank Reshi Shanmuganathan for help with identifying orthologs. We acknowledge the Graduate School Life Science Munich (LSM) for their valuable support to S.P.C. We would also like to thank Prof. Yutaka Sato and Mr. Hiroyasu Furumi at the National Institute of Genetics, Japan, for providing wild rice material, and Chisato Goda (Yamagata University, Japan) for technical support.

FUNDING

This work was supported by the Deutsche Forschungsgemeinschaft (DFG; grant no. 457739273 (C.B.) and by JSPS KAKENHI Grant Numbers 20H02922 (K.O.) and 23H02148 (T.T.). For computational analyses, we used the BioHPC-Genomics compute cluster at the Leibniz Rechenzentrum (DFG; grant no. 450674345).

1185 SUPPLEMENTARY MATERIAL

1186 **Supplementary Figure 1: Phylogenetic analysis based on CPS4 amino acid**
1187 **sequence.**

1188 **Supplementary Figure 2: Phylogenetic analysis based on KSL4 amino acid**
1189 **sequence.**

1190 **Supplementary Figure 3: Phylogenetic analysis based on MAS amino acid**
1191 **sequences.**

1192 **Supplementary Figure 4: Phylogenetic analysis based on CYP99A amino acid**
1193 **sequences.**

1194 **Supplementary Figure 5: Microsynteny of the MBGC between *O. sativa* and**
1195 **species and sub-genomes lacking a MBGC**

1196 **Supplementary Figure 6: Synteny between *O. coarctata* sub-genome LL and *E.***
1197 ***crus-galli* sub-genome CC showing the lack of synteny between the genomic**
1198 **region containing the MBGC in *O. coarctata* (Chr4) and *E. crus-galli* (Chr4 sub-**
1199 **genome CH) at different magnifications.**

1200 **Supplementary Figure 7. Phylogenetic relationship between the *Poaceae***
1201 **species used in this study.**

1202 **Supplementary Figure 8: Cladogram representing the amino-acid-sequence**
1203 **maximum likelihood tree with the best-fit model selected by ModelFinder**
1204 **representing the relationship between the orthogroup containing *O. coarctata***
1205 **CYP76L11.**

1206 **Supplementary Figure 9: Expression of the momilactone biosynthetic orthologs**
1207 **within and outside the MBGC in *O. officinalis* (a) and *O. coarctata* (b).**

1208 **Supplementary Figure 10: Amino acid sequence alignment.**

1209 **Supplementary Figure 11: Prevalence of the nonsense G-to-A polymorphism in**
1210 **OoKSL4-2 cDNA clones at the population level.**

1211 **Supplementary Figure 12: Mass spectra of peaks identified.**

1212 **Supplementary Figure 13: Microsynteny analysis of the genomic regions**
1213 **containing the MBGC-like.**

1214

1215 **Supplementary Table 1. Key statistics on the reference genome assemblies**
1216 **used in this study.**

1217 **Supplementary Table 2. Scaffold and positional information on the orthologs of**
1218 **MBGC genes shown in Figure 1.**

SUPPLEMENTARY FIGURES

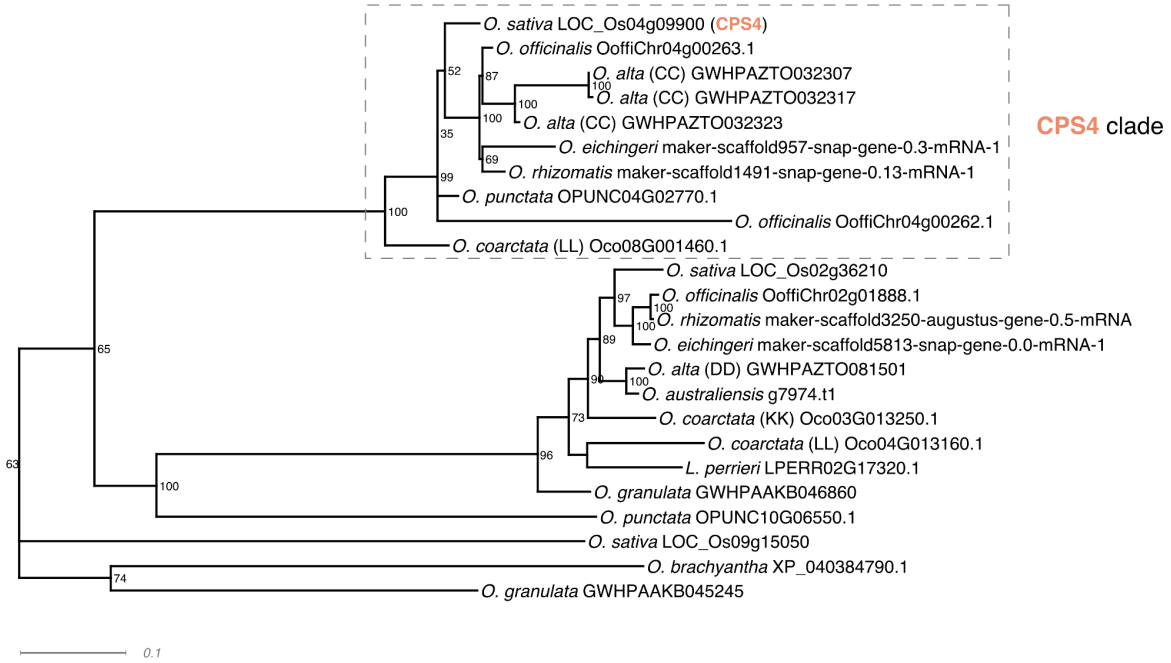

Supplementary Figure 1. Phylogenetic analysis based on CPS4 amino acid sequence. Maximum likelihood tree with the best-fit model selected by ModelFinder for the orthogroup containing *O. sativa* CPS4 (LOC_Os04g09900) in *O. sativa*, *O. punctata*, *O. officinalis*, *O. eichingeri*, *O. rhizomatis*, *O. alta*, *O. australiensis*, *O. coarctata*, *O. brachyantha*, *O. granulata* and *L. perrieri*. Numbers represent 1000 replicates of ultrafast bootstrapping. Dashed rectangle highlights the CPS4 clade, which contains orthologs potentially involved in momilactones biosynthesis and clustered in *Oryza* species.

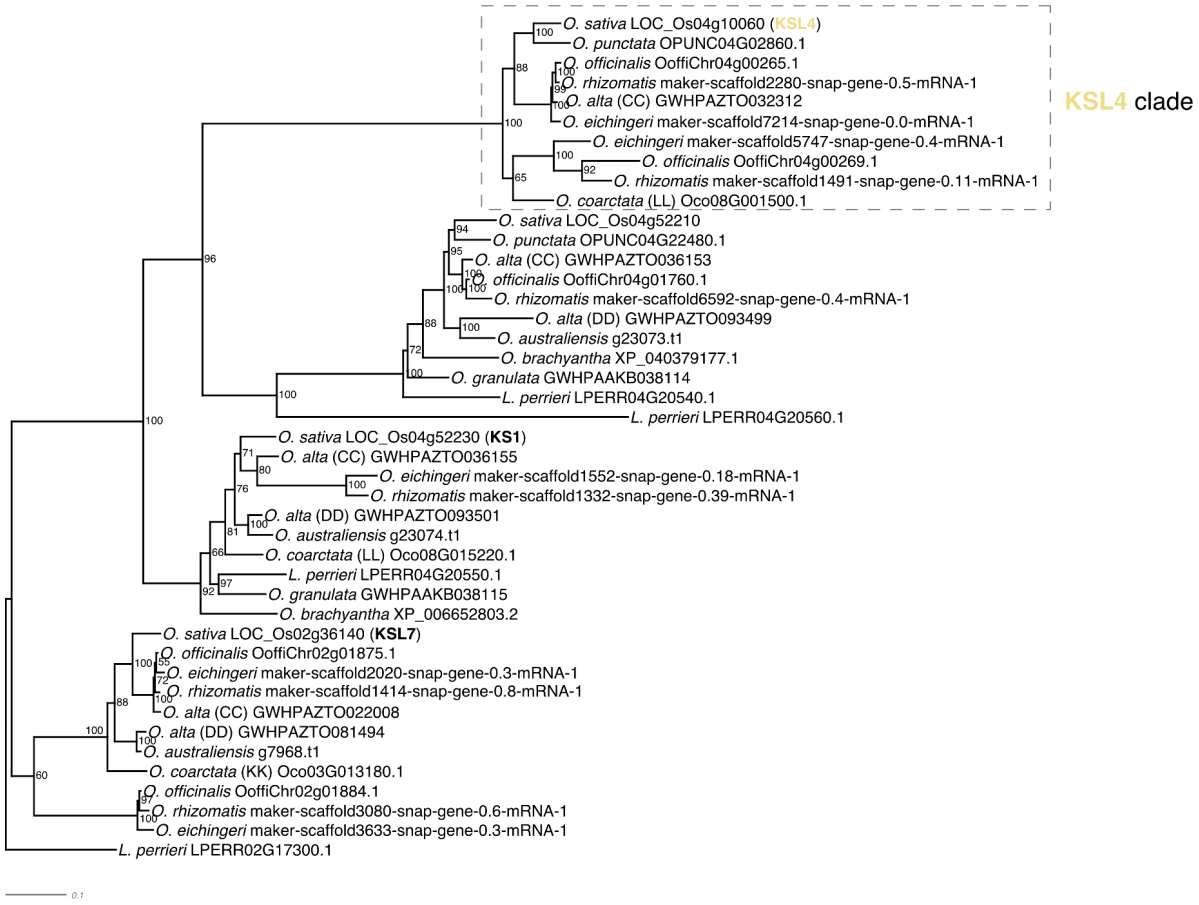

Supplementary Figure 2. Phylogenetic analysis based on KSL4 amino acid sequence. Maximum likelihood tree with the best-fit model selected by ModelFinder for the orthogroup containing *O. sativa* KSL4 (LOC_Os04g10060) in *O. sativa*, *O. punctata*, *O. officinalis*, *O. eichingeri*, *O. rhizomatis*, *O. alta*, *O. australiensis*, *O. coarctata*, *O. brachyantha*, *O. granulata* and *L. perrieri*. Numbers represent 1000 replicates of ultrafast bootstrapping. Dashed rectangle highlights the KSL4 clade, which contains orthologs potentially involved in momilactones biosynthesis and clustered in *Oryza* species.

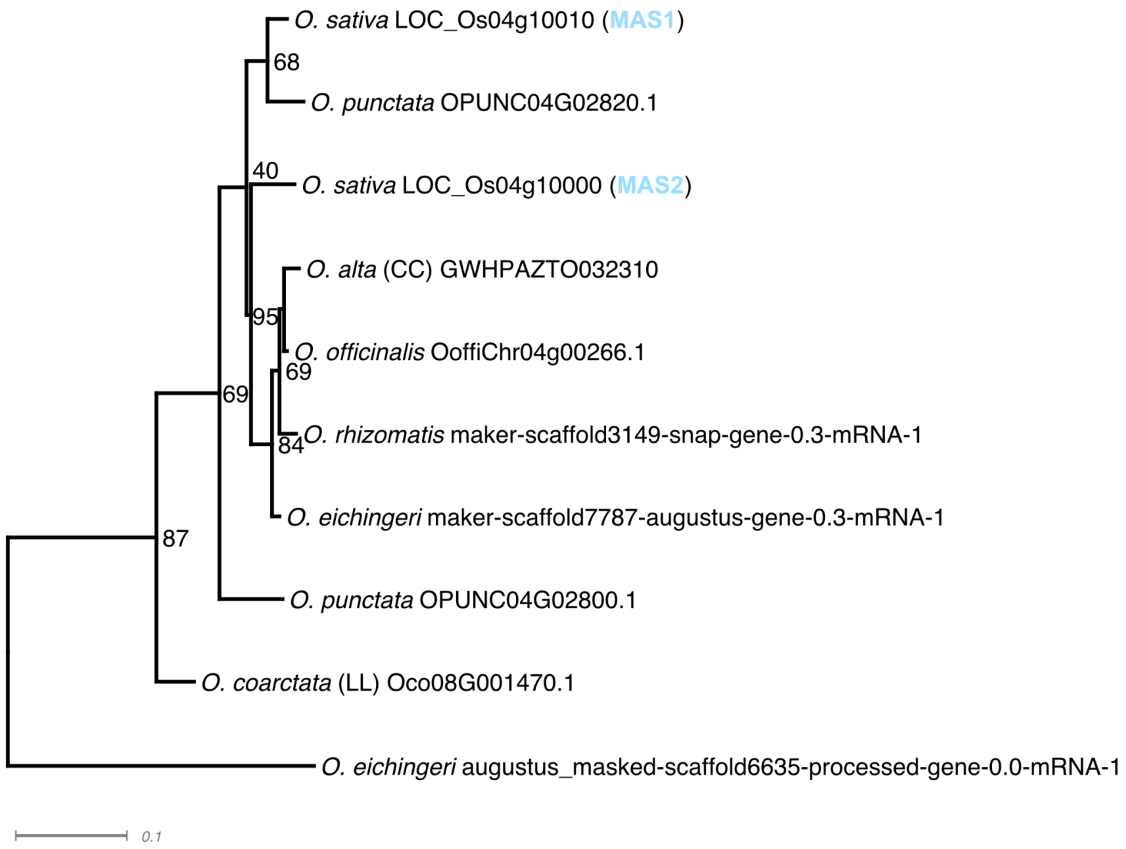

Supplementary Figure 3. Phylogenetic analysis based on MAS amino acid sequences. Maximum likelihood tree with the best-fit model selected by ModelFinder for the orthogroup containing *O. sativa* MAS1 and MAS2 (LOC_Os04g10010, LOC_Os04g10000) in *O. sativa*, *O. punctata*, *O. officinalis*, *O. eichingeri*, *O. rhizomatis*, *O. alta*, *O. australiensis*, *O. coarctata*, *O. brachyantha*, *O. granulata* and *L. perrieri*. Numbers represent 1000 replicates of ultrafast bootstrapping. Since this orthogroup consisted of a small number of genes, we considered all of them as potentially involved in momilactone biosynthesis and clustered.

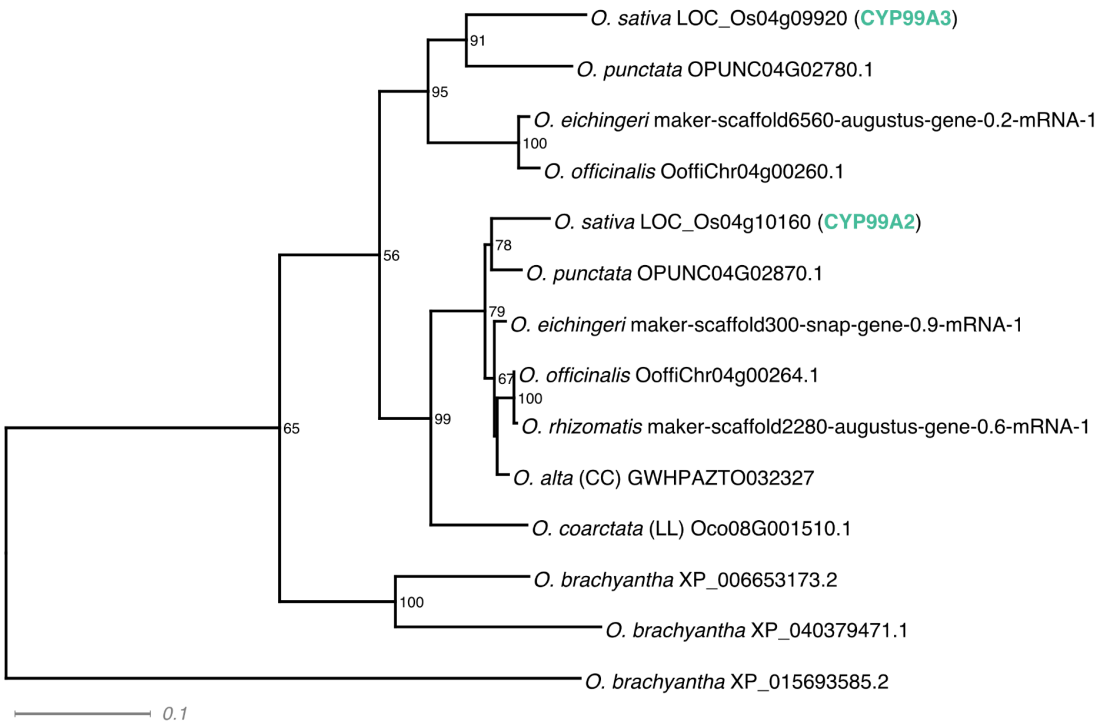

Supplementary Figure 4. Phylogenetic analysis based on CYP99A amino acid sequences. Maximum likelihood tree with the best-fit model selected by ModelFinder for the orthogroup containing *O. sativa* CYP99A2 and CYP99A3 (LOC_Os04g10160, LOC_Os04g09920) in *O. sativa*, *O. punctata*, *O. officinalis*, *O. eichingeri*, *O. rhizomatis*, *O. alta*, *O. australiensis*, *O. coarctata*, *O. brachyantha*, *O. granulata* and *L. perrieri*. Numbers represent 1000 replicates of ultrafast bootstrapping. Since this orthogroup consisted of a small number of genes, we considered all of them as potentially involved in momilactone biosynthesis and clustered.

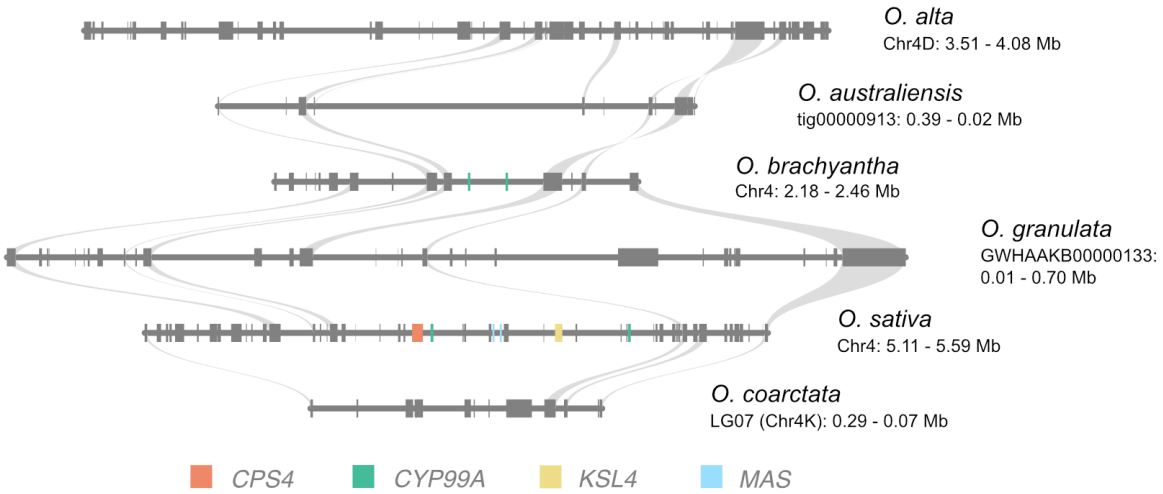

Supplementary Figure 5. **Microsynteny of the MBGC between *O. sativa* and species and sub-genomes lacking a MBGC.** *O. alta* sub-genome DD was used as anchor species. The region was not further expanded given the fragmented nature of the assemblies for *O. australiensis* and *O. granulata*. Coloured rectangles represent the momilactone biosynthetic genes. Grey lines connect orthologs.

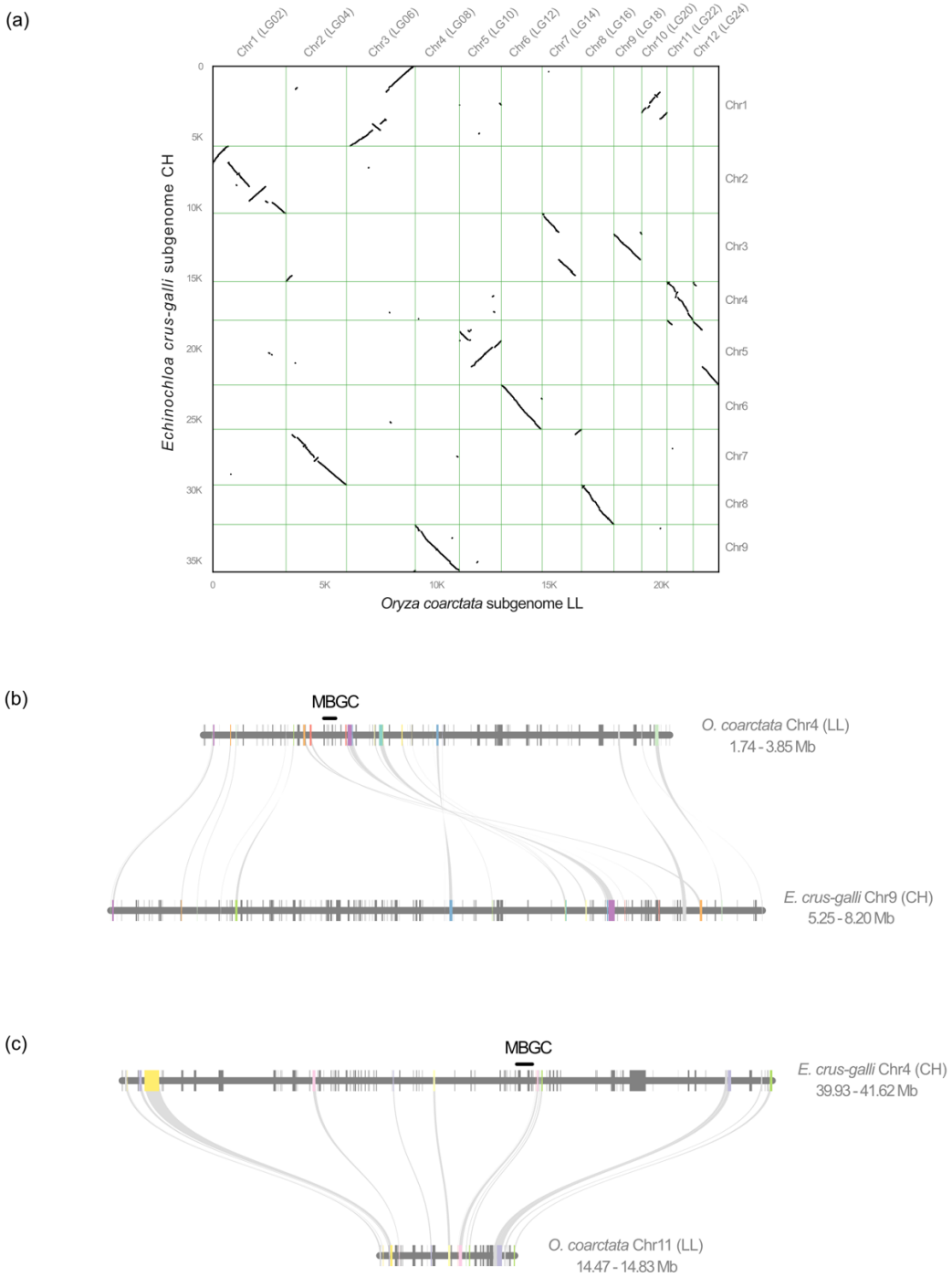

Supplementary Figure 6. Synteny between *O. coarctata* sub-genome LL and *E. crus-galli* sub-genome CH showing the lack of synteny between the genomic region containing the MBGC in *O. coarctata* (Chr4) and *E. crus-galli* (Chr4 sub-genome CH). a) Dot plot showing whole-genome pairwise synteny between *O. coarctata* sub-genome LL and *E. crus-galli* sub-genome CH **b)** Synteny between the genomic region of *O. coarctata* containing MBGC (Chr4 LL) and its syntenic block in *E. crus-galli* sub-genome CH (Chr9). **c)** Synteny between the genomic region of *E. crus-galli* containing MBGC (Chr4 CH) and its syntenic block in *O. coarctata* sub-genome LL (Chr11). In (**b)** and **(c)**, grey lines connect the respective orthologs, and the black horizontal line indicates where the MBGC is located on each species.

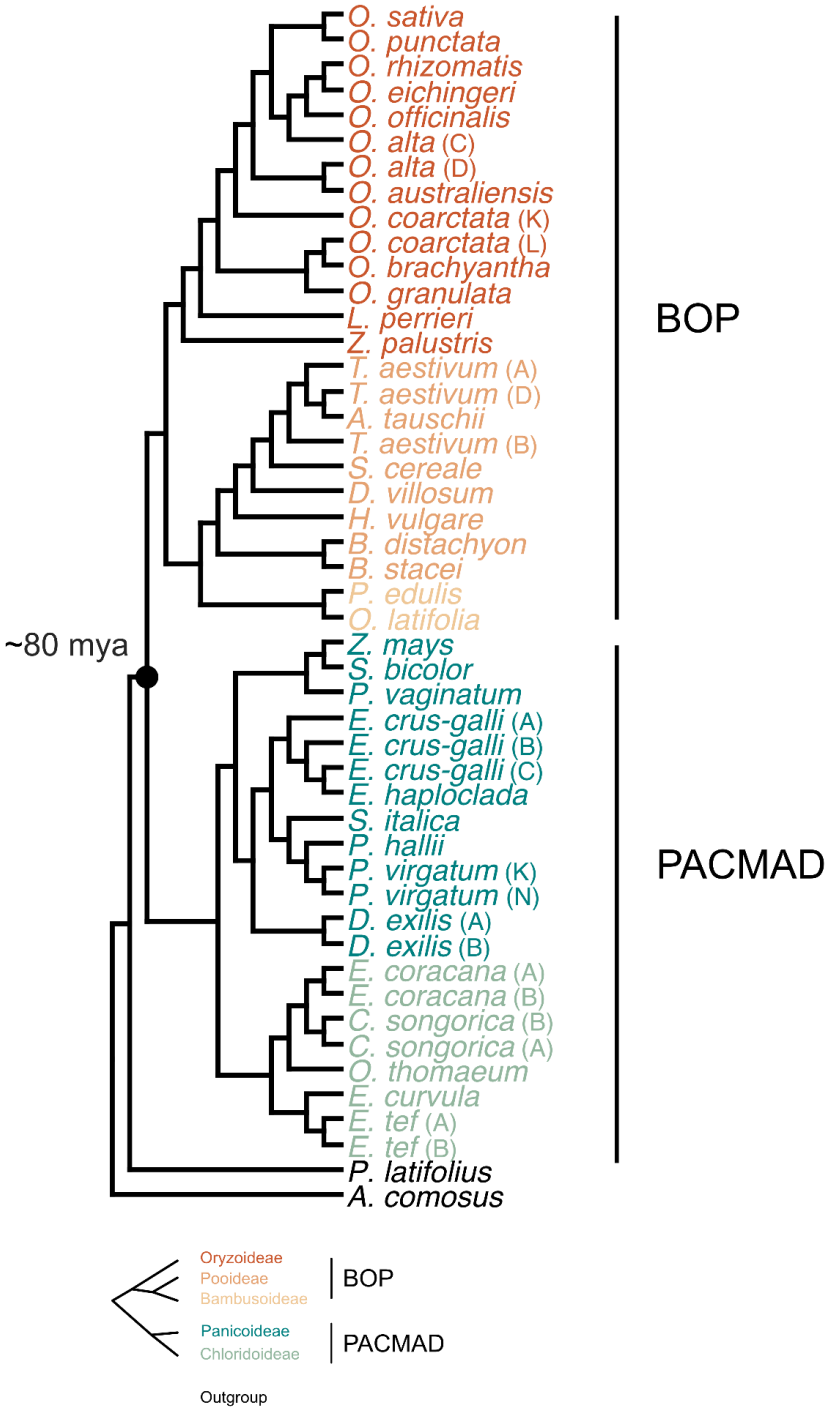

Supplementary Figure 7. Phylogenetic relationship between the Poaceae species used in this study. The tree was inferred with the OrthoFinder algorithm STAG (Emms and Kelly, 2018) that uses all the species tree inferred from all orthogroups. *P. latifolius* (Poaceae) outgroup of core Poaceae (BOP and PACMAD), *A. comosus*, outgroup of Poaceae.

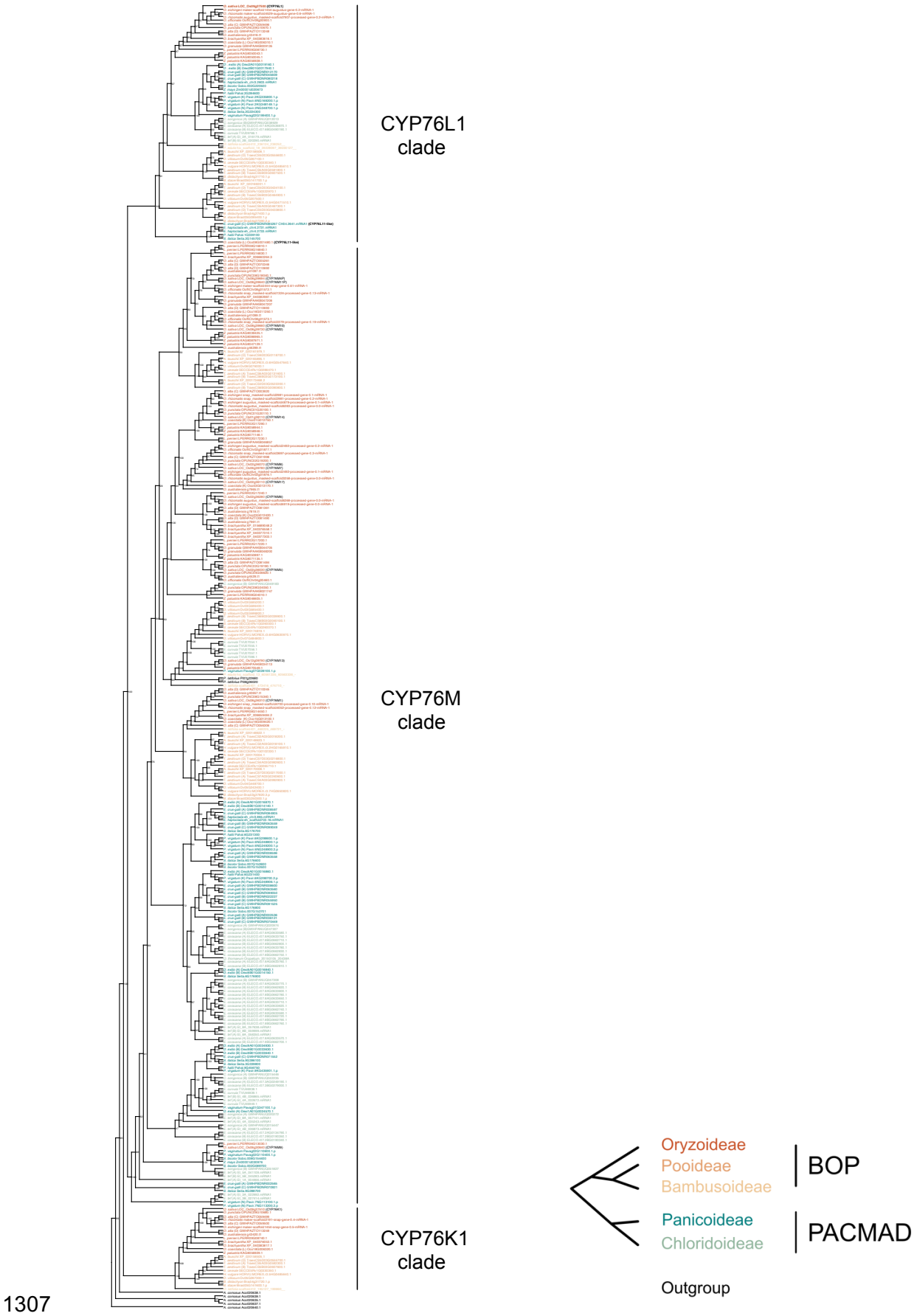
CYP76L1
clade
CYP76M
clade
CYP76K1
clade
1307
Oryzoideae
Pooideae
Bambusoideae
BOP
Panicoideae
Chloridoideae
PACMAD
Outgroup

1308 **Supplementary Figure 8. Cladogram representing the amino-acid-sequence maximum likelihood**
1309 **tree with the best-fit model selected by ModelFinder representing the relationship between the**
1310 **orthogroup containing *O. coarctata* CYP76L11.** The claudogram contains the CYP76K, CYP76L and
1311 CYP76M clades of 37 Poaceae species belonging to the subfamilies Oryzoideae, Pooideae,
1312 Bambusoideae, Panicoideae and Chloridoideae. The names of the different rice CYPs were taken from
1313 https://funricegenes.github.io/cytochrome_P450_monooxygenase_superfamily/. The phylogenetic
1314 relation between these subfamilies is represented in the bottom-right graph.
1315

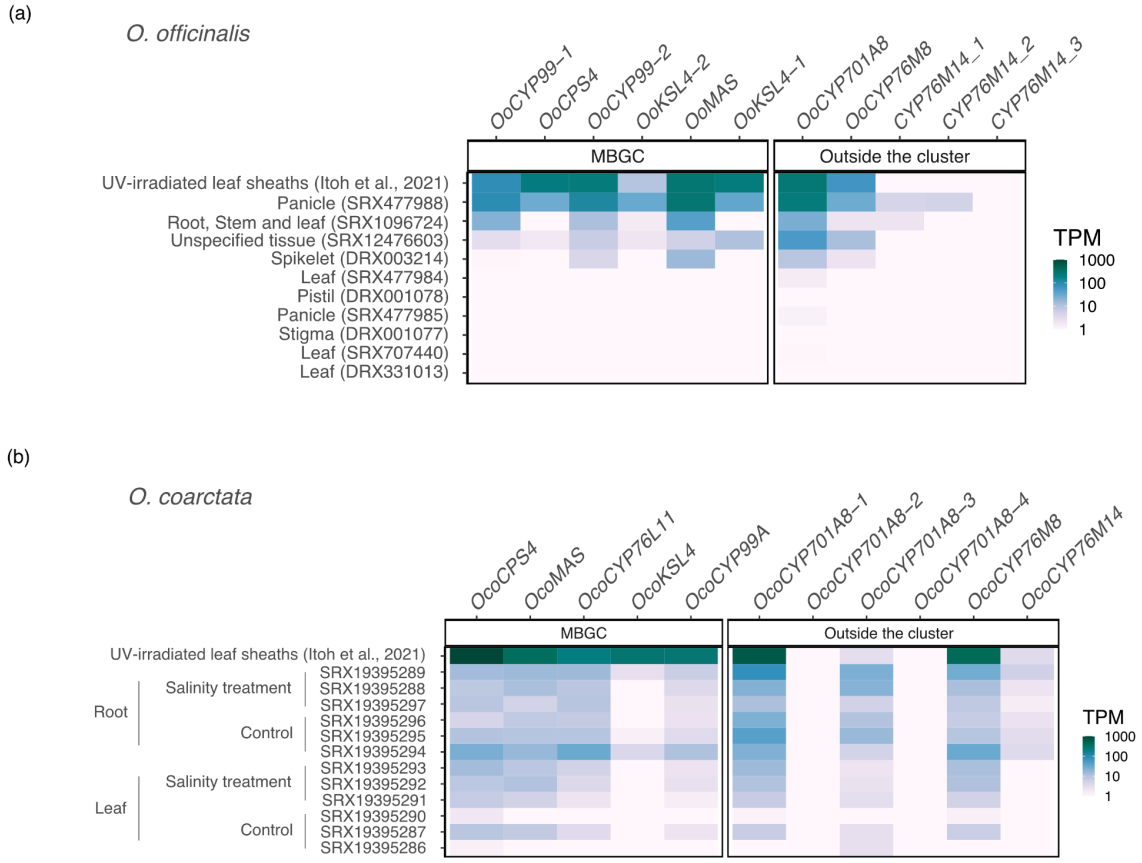

Supplementary Figure 9. Expression of the momilactone biosynthetic orthologs within and outside the MBGC in a) *O. officinalis* and b) *O. coarctata*. The expression is represented as transcripts per million (TPM) and the colour is in logarithmic scale. The RNA-seq datasets were publicly available RNA-seq (see y axis on each heatmap) and these cover different tissues and treatments. Notice that the genes belonging to the MBGC are represented in the same order as in the cluster.

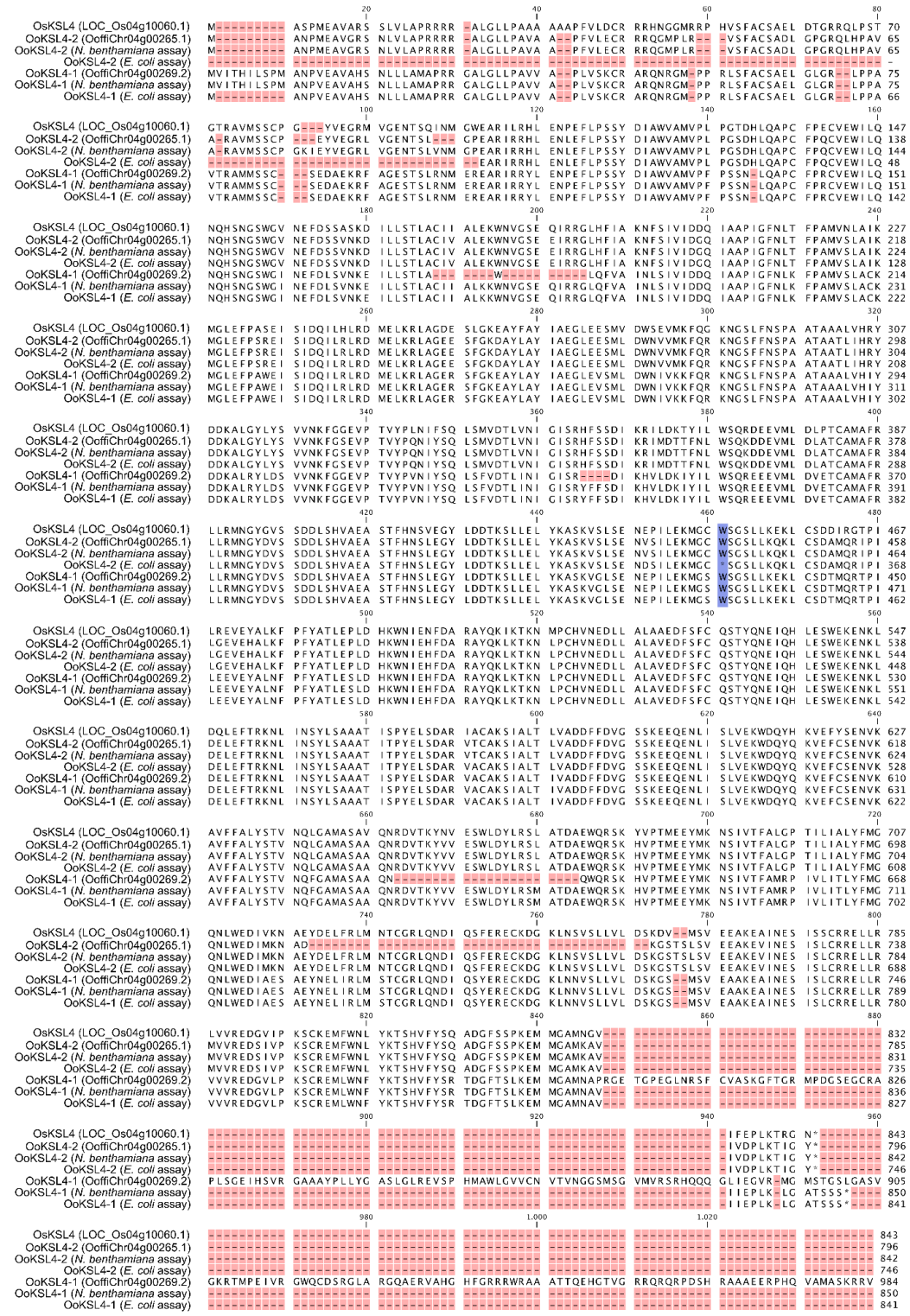

Supplementary Figure 10. Amino acid sequence alignment of KSL4 orthologs. The alignment includes KSL4 from *O. sativa* (OsKSL4), its orthologs in *O. officinalis* from the annotation (KSL4-2: OoffiChr04g00265.1; KSL4-1: OoffiChr04g00269.2) and the cloned sequences used in *N. benthamiana* and *E. coli* assays. The position of the W445 clonal *de novo* mutation is highlighted in OoKSL4-2 (position assigned using the full length *OoKSL4-2* sequence cloned for the *N. benthamiana* transient expression as the reference sequence).

(a)

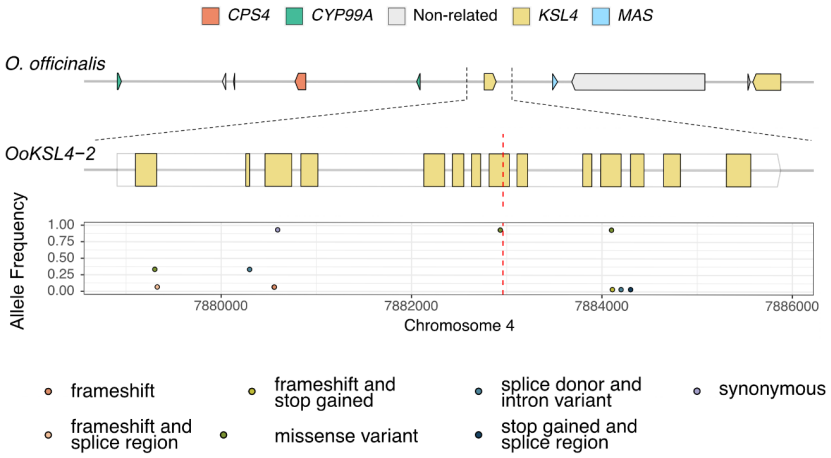

(b)

```
OoKSL4-2-W0566      TCAGTTTATCAGAAAATGACTCAATCCTAGAGAAAATGGGTTGTTGGTCAGGTAGCTTAT
OoKSL4-2-W0614      TCAGTTTATCAGAAAATGACCCAATCCTAGAGAAAATGGGTTGTTGGTCAGGTAGATTAT
OoKSL4-2-W1200      TCAGTTTATCAGAAAATGACTCAATCCTAGAGAAAATGGGTTGTTGGTCAGGTAGCTTAT
OoKSL4-2-W0002      TCAGTTTATCAGAAAATGTCTCAATCCTAGAGAAAATGGGTTGTTGGTCAGGTAGCTTAT
OoKSL4-2-W1252      TCAGTTTATCAGAAAATGACTCAATCCTAGAGAAAATGGGTTGTTGGTCAGGTAGCTTAT
OoKSL4-2-W1131      TCAGTTTATCAGAAAATGACTCAATCCTAGAGAAAATGGGTTGTTGGTCAGGTAGCTTAT
OoKSL4-2_cDNA       TCAGTTTATCAGAAAATGACTCAATCCTAGAGAAAATGGGTTGTTAGTCAGGTAGCTTAT
                      ****************** * ************************ ********* ****

OoKSL4-2-W0566      TGAAACAAAAATTGTGCTCCGATGCCATGCAAAGAATACCAATCCTTGGAGAGGTGCGTG
OoKSL4-2-W0614      TGAAACAAAAATTGTGCTCCGATGCCATGCAAAGAATACCAATCCTTGGTGAGGTGCGTG
OoKSL4-2-W1200      TGAAACAAAAATTGTGCTCCGATGCCATGCAAAGAATACCAATCCTTGGAGAGGTGCGTG
OoKSL4-2-W0002      TGAAACAAAAATTGTGCTCCGATGCCATGCAAAGAATACCAATCCTTGGAGAGGTGCGTG
OoKSL4-2-W1252      TGAAACAAAAATTGTGCTCCGATGCCATGCAAAGAATACCAATCCTTGGAGAGGTGCGTG
OoKSL4-2-W1131      TGAAACAAAAATTGTGCTCCGATGCCATGCAAAGAATACCAATCCTTGGAGAGGTGCGTG
OoKSL4-2_cDNA       TGAAACAAAAATTGTGCTCCGATGCCATGCAAAGAATACCAATCCTTGGAGAG-------
                      ************************************************* ***

OoKSL4-2-W0566      CATGAAACTCATGATCCCCATTTCAGTTGAAATTTATGTTTACATTCGATTCAGTTGGTT
OoKSL4-2-W0614      CATGAAACTCATGATCCCCATTTCAGTTGAAATTTATGTTTACATTCGATTCAGTTAGTT
OoKSL4-2-W1200      CATGAAACTCATGATCCCCATTTCAGTTGAAATTTATGTTTACATTCGATTCAGTTGGTT
OoKSL4-2-W0002      CATGAAACTCATGATCCCCATTTCAGTTGAAATTTATGTTTACATTCGATTCAGTTGGTT
OoKSL4-2-W1252      CATGAAACTCATGATCCCCATTTCAGTTGAAATTTATGTTTACATTCGATTCAGTTGGTT
OoKSL4-2-W1131      CATGAAACTCATGATCCCCATTTCAGTTGAAATTTATGTTTACATTCGATTCAGTTGGTT
OoKSL4-2_cDNA       ------------------------------------------------------------

OoffKSL4-2-W0566      TTTCTCATTTCAGGTCGAACATGCTCTCAAATTTCCATTTTATGCCACGCTT
OoffKSL4-2-W0614      TTTCTCATTTCAGGTAGAACATGCTCTCAAATTTCCATTTTATGCCACGCTT
OoffKSL4-2-W1200      TTTCTCATTTCAGGTCGAACATGCTCTCAAATTTCCATTTTATGCCACGCTT
OoffKSL4-2-W0002      TTTCTCATTTCAGGTCGAACATGCTCTCAAATTTCCATTTTATGCCACGCTT
OoffKSL4-2-W1252      TTTCTCATTTCAGGTCGAACATGCTCTCAAATTTCCATTTTATGCCACGCTT
OoffKSL4-2-W1131      TTTCTCATTTCAGGTCGAACATGCTCTCAAATTTCCATTTTATGCCACGCTT
OoffKSL4-2_cDNA       -------------GTCGAACATGCTCTCAAATTTCCATTTTATGCCACGCTT
                                  ** ************************************
```

Supplementary Figure 11. Prevalence of the nonsense G-to-A polymorphism in *OoKSL4-2* cDNA clones at the population level. a) The biosynthetic gene cluster (MBGC) from *O. officinalis*. Middle panel shows a magnification of the *OoKSL4-2* locus where the yellow filled rectangles represent exons of *OoKSL4-2*. Bottom panel shows the allele frequency of single nucleotide polymorphisms (SNPs) with a potential disruptive effect on *OoKSL4-2* from 15 *O. officinalis* accessions. The SNPs represented have allele frequency > 0.2 or a putative impact annotated as 'high'. The red dashed line indicates the position of the G-to-A transition in the original cDNA clone, which is absent at the population level. **b)** Comparison of genome sequences of several *O. officinalis* accessions. The underlined codon indicates the mutation detected in the cDNA clones of OoKSL4-2 (W0002), which is absent in other accessions and in a different W0002 batch.

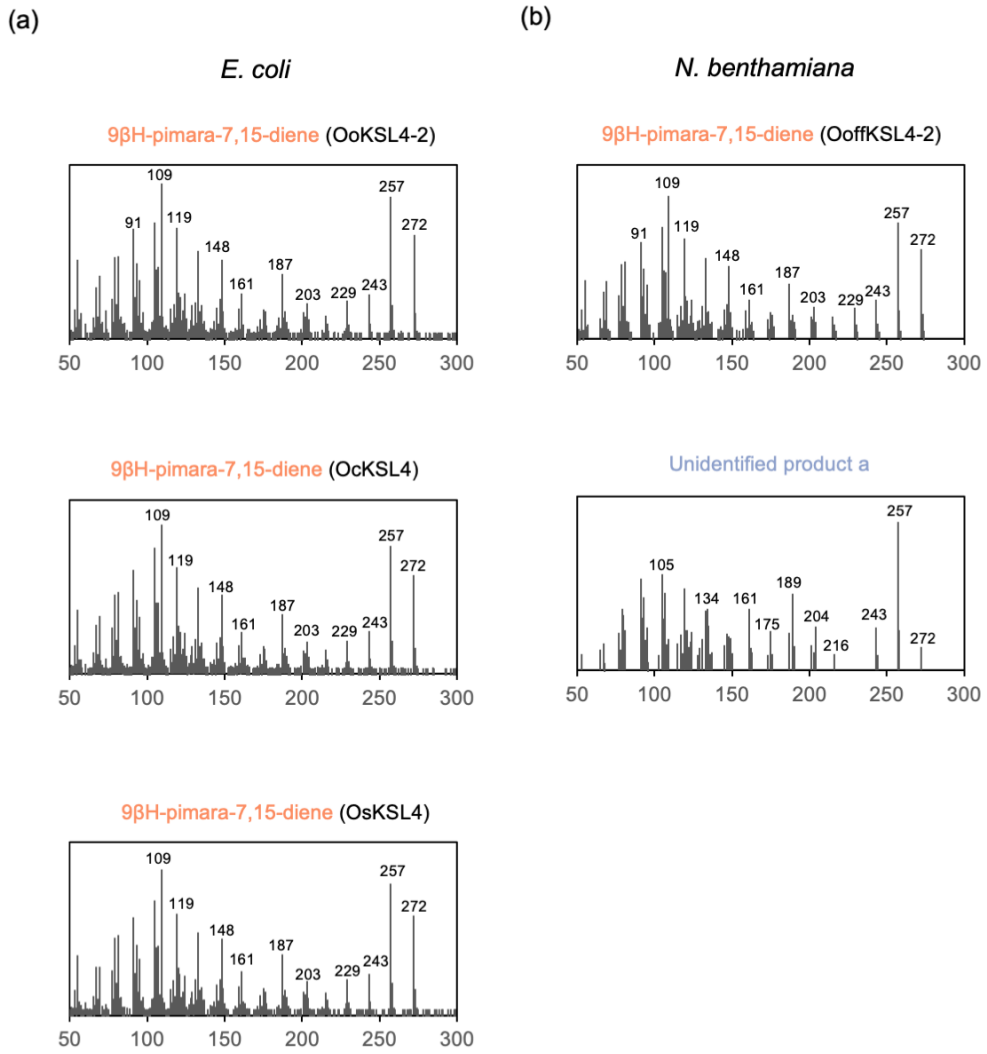

Supplementary Figure 12. Mass spectra of peaks identified in *E. coli* metabolic engineering system (**a**) and *Nicotiana benthamiana* transient expression system **(b)**.

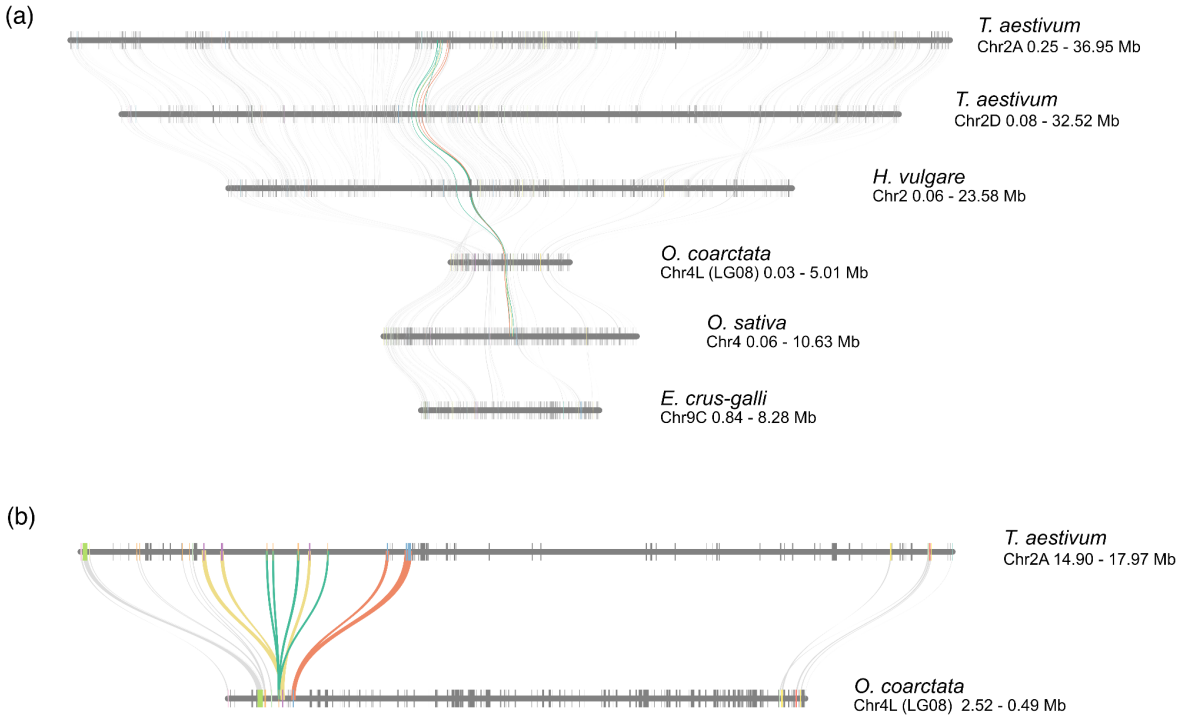

Supplementary Figure 13. Microsynteny analysis of the genomic regions containing the MBGC-like from **a)** *Triticum aestivum* (wheat), *Hordeum vulgare* and the MBGC from *O. coarctata* and *O. sativa*. **b)** Magnification of the genomic region containing the MBGC-like and the MBGC in *T. aestivum* (sub-genome A) and *O. coarctata* showing the synteny between the flanking regions of both BGCs. Coloured lines represent MBGC-like orthologs and grey lines connect the respective orthologs.

1354 # SUPPLEMENTARY TABLES

Species	Version	Genome type	Assembly Size (Mb)	Annotated Loci	Scaffold N50 (Mb)	Complete BUSCOs (%)	Reference
O. sativa	v7.0	AA	375	42189	30	95	Phytozome
O. punctata	v1.2	BB	394	31762	13	97,2	Stein et al., 2018
O. officinalis	GCA_008326285.1	CC	584	29930	0,51	94,6 or 98	Shenton et al., 2020
O. rhizomatis		CC	559	32083	0,082	90,8	Shenton et al., 2020
O. eichingeri		CC	471	3103	0,064	91,6	Shenton et al., 2020
O. alta	GWHAZTO00000000	CCDD	895	99312	37	98,2	Yu et al., 2021
		sub-genome CC	441	52861			
		sub-genome DD	435	46388			
O. australiensis	GCA_019925245.2 (MQ-UA-ANU_Oaus-KR_2.0) - Contig annotation	EE	996	51057	1,9	91,9	Phillips et al., 2022
O. coarctata			556	45571	23,1	96,22	Zhao et al., 2023
		KK	271				
		LL	261				
O. brachyantha	GCF_000231095.2 (ObraRS2)	FF	261	32038	1,6	95,9	Chen et al., 2013
O. granulata	GWHAAKB00000000	GG	737	40131	0,92	96,53	Shi et al., 2020
Leersia perrieri	v1.4	outgroup	267		8,7	97,6	Stein et al., 2018

1355

1356 **Supplementary Table 1. Key statistics on the reference genome assemblies used in this study.**

Species	MBGC gene	MBGC ortholog	Chr	Orientation	Start	End	Annotation
O. sativa	CPS4	LOC_Os04g09900	Chr4	+	5318060	5326427	Phytozome
O. punctata		OPUNC04G02770	4	+	4522865	4529604	Stein et al., 2018
O. officinalis		OoffiChr04g00263	OoffiChr04	-	7769720	7775970	Shenton et al., 2020
O. eichingeri		maker-scaffold957-snap-gene-0.3	scaffold957	-	62784	69194	
O. rhizomatis		maker-scaffold1491-snap-gene-0.13	scaffold1491	-	71863	78506	
O. alta		GWHPAZTO032307 (OalC04g148840)	GWHAZTO00000004	+	4117988	4123024	Yu et al., 2021
		GWHPAZTO032317 (OalC04g148720)	GWHAZTO00000004	-	4469590	4477143	
		GWHPAZTO032323 (OalC04g148850)	GWHAZTO00000004	-	4590053	4596229	
O. coarctata		Oco08G001460	LG08	+	2283517	2288401	Zhao et al., 2023
O. sativa	KSL4	LOC_Os04g10060	Chr4	-	5428338	5434028	Phytozome
O. punctata		OPUNC04G02860	4	-	4651798	4657918	Stein et al., 2018
O. officinalis		OoffiChr04g00265 (KSL4-2)	OoffiChr04	+	7878906	7885876	Shenton et al., 2020
		OoffiChr04g00269 (KSL4-1)	OoffiChr04	-	8034073	8050226	
O. eichingeri		maker-scaffold7214-snap-gene-0.0	scaffold7214	-	6323	12766	
		maker-scaffold5747-snap-gene-0.4	scaffold5747	-	1770	5809	
O. rhizomatis		maker-scaffold2280-snap-gene-0.5	scaffold2280	-	19912	26338	
		maker-scaffold1491-snap-gene-0.11	scaffold1491	-	46688	48700	
O. alta		GWHPAZTO032312 (OalC04g148800)	GWHAZTO00000004	-	4220817	4228485	Yu et al., 2021
O. coarctata		Oco08G001500	LG08	-	2320899	2325854	Zhao et al., 2023
O. sativa	MAS	LOC_Os04g10010 (MAS1)	Chr4	-	5385722	5387215	Phytozome
		LOC_Os04g10000 (MAS2)	Chr4	-	5380095	5381565	
O. punctata		OPUNC04G02820	4	-	4619323	4620404	Stein et al., 2018
		OPUNC04G02800	4	+	4607713	4609250	
O. officinalis		OoffiChr04g00266	OoffiChr04	+	7920441	7921389	Shenton et al., 2020
O. eichingeri		maker-scaffold7787-augustus-gene-0.3	scaffold7787	-	8229	9170	
		augustus_masked-scaffold6635-processed-gene-0.0	scaffold6635	-	7865	8407	
O. rhizomatis		maker-scaffold3149-snap-gene-0.3	scaffold3149	-	49186	50134	
O. alta		GWHPAZTO032310 (OalC04g148820)	GWHAZTO00000004	-	4161740	4164110	Yu et al., 2021
O. coarctata		Oco08G001470	LG08	-	2297380	2298521	Zhao et al., 2023
O. sativa	CYP99A	LOC_Os04g09920 (CYP99A3)	Chr4	-	5332329	5334479	Phytozome
		LOC_Os04g10160 (CYP99A2)	Chr4	+	5484768	5486773	
O. punctata		OPUNC04G02780	4	-	4537911	4539644	Stein et al., 2018
		OPUNC04G02870	4	+	4692353	4694580	
O. officinalis		OoffiChr04g00260	OoffiChr04	+	7667067	7669495	Shenton et al., 2020
		OoffiChr04g00264	OoffiChr04	-	7839962	7841978	
O. eichingeri		maker-scaffold6560-augustus-gene-0.2	scaffold6560	+	5202	7197	
		maker-scaffold300-snap-gene-0.9	scaffold300	+	26448	28078	
O. rhizomatis		maker-scaffold2280-augustus-gene-0.6	scaffold2280	+	64230	65860	
O. alta		GWHPAZTO032327 (OalC04g148580)	GWHAZTO00000004	+	4644874	4645779	Yu et al., 2021
O. coarctata		Oco08G001510	LG08	+	2336194	2338065	Zhao et al., 2023
O. brachyantha		XP_006653173 (gene-LOC102721730)	NC_023166.2	-	2359703	2361535	Chen et al., 2013
O. brachyantha		XP_040379471 (gene-LOC102721444)	NC_023166.2	-	2330641	2332473	
O. sativa	CYP701A8	LOC_Os06g37300	Chr6	-	22020840	22028146	Phytozome
O. officinalis		OoffiChr06g01688	OoffiChr06	-	36504697	36512007	Shenton et al., 2020
O. coarctata		Oco11G011450 (OcCYP701A8-1)	LG11	-	16913203	16920158	Zhao et al., 2023
		Oco12G011620 (OcCYP701A8-2)	LG12	-	15919197	15926532	
		Oco12G011590 (OcCYP701A8-3)	LG12	-	15872696	15874541	
		Oco12G011610 (OcCYP701A8-4)	LG12	-	15894445	15896283	
O. sativa	CYP76M8	LOC_Os02g36070	Chr2	+	21690378	21692186	Phytozome
O. officinalis		OoffiChr02g01877	OoffiChr02g01877	-	38647795	38649297	Shenton et al., 2020
O. coarctata		Oco03G013170	LG03	+	18711059	18712555	Zhao et al., 2023
O. sativa	CYP76M14	LOC_Os01g38110	Chr1	-	21342129	21344086	Phytozome
O. officinalis		CYP76M14_1	OoffiChr01	+	31900002	31901558	This study
		CYP76M14_2	OoffiChr01	+	32851333	32852889	This study
		CYP76M14_3	OoffiChr01	+	30558655	30560211	This study
O. coarctata		Oco01G012750	LG01	-	17503624	17505405	Zhao et al., 2023

Supplementary Table 2. Scaffold and positional information on the orthologs of MBGC genes shown in Figure 1.